Master of Environmental Engineering

Adsorption of tetracycline from water by magnetic biochar from pine bark

**The Graduate School
of the University of Ulsan**

Department of Civil and Environmental Engineering

Adsorption of tetracycline from water by magnetic biochar from pine bark

Supervisor: Hung-Suck Park

A Dissertation

Submitted to
The Graduate School of the University of Ulsan in Partial
Fulfillment of the Requirements for the Degree of

Master of Environmental Engineering
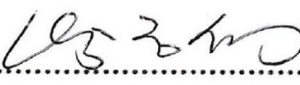
by

Urjinlkham Ryenchindorj

Department of Civil and Environmental Engineering
University of Ulsan, Korea
February 2020

Adsorption of tetracycline from water by magnetic biochar from pine bark

This certifies that the master dissertation

of Urjinlkham Ryenchindorj is approved.

Committee Chairman:..................................

Prof. Byeong-Kyu Lee

Committee Member:..................................

Prof. Jongmuk Won

Committee Member:..................................

Prof. Hung-Suck Park

Department of Civil and Environmental Engineering

Ulsan, Korea

February, 2020

ACKNOWLEDGEMENTS

DEDICATION

I would like to dedicate this thesis to my beloved grandfather who taught me the love, being loyal and patience.

ABSTRACT

The occurrence of tetracycline (TC) in water systems ends up in water cycle which leads to unnecessary consumption of the antibiotic by humans and animals. This leads to the weakening of the immune system of the human body. This calls for the removal of the antibiotic from water.

This work was performed to evaluate low cost adsorbent, pine bark biochar (PBB), to remove tetracycline from aqueous solution via adsorption pathway. Pine bark biochar was prepared using pine bark from forest waste. The pyrolysis of the raw material was performed in tubular furnace at $600\,^{\circ}C$ in nitrogen atmosphere. The PBB, hence obtained, was modified via co-precipitation of aqueous ferric and ferrous ion solution to obtain magnetic pine bark biochar (M-PBB). Batch adsorption experiments were conducted to examine the adsorption removal of TC by PBB and M-PBB on the impact of pH, dosage, and temperature. The aqueous concentrations of TC were determined by UV-VIS spectrophotometer. The adsorbents were characterized by SEM/EDX, TGA and pH_{pzc}. The adsorption mechanism was evaluated by fitting widely used Langmuir, Freundlich, Temkin and Dubinin-Radushkevich (D-R) isotherms. Also, the experimental data are analyzed by kinetics models (pseudo first order, pseudo second order, intra-particle diffusion and Elovich) and thermodynamics (Gibbs free energy, enthalpy and entropy).

Characterization of the materials showed that iron oxide was prevalent in M-PBB. SEM images exhibited coating of iron oxide on the surface of biochar. EDX supported the findings of SEM micrographs. TGA approximated ~27% iron oxide content in the M-PBB.

When compared to PBB, M-PBB exhibited higher adsorption capacity for tetracycline (from aqueous solutions). At similar experimental conditions (i.e. tetracycline initial concentration: 25 mg/L, pH 6, and 16 hrs contact time), the equilibrium adsorption capacity (q_e) was found to be 2.1 mg/g and 10.5 mg/g for PBB and M-PBB, respectively. The maximum adsorption capacity (q_m) of M-PBB was 15.3 mg/g. The highest adsorption was observed at pH 4-6 owing to ionization of tetracycline with respect to pH. A high correlation co-efficient ($R^2 \approx 0.9$) of Freundlich isotherm postulated multilayer sorption of tetracycline on M-PBB at pH 6 and 9. The kinetic studies showed the pseudo-second-order was more suitable for indicating adsorption of TC molecules on the surface to be the rate limiting step in the process. Thermodynamic analysis was discovered that adsorption process is favorable, spontaneous and endothermic at studied temperature (293 – 323 K). M-PBB could be a having potential for removal of TC from water as a low cost and easy to removable adsorbent.

Keywords: Pine bark biochar, Magnetic pine bark biochar, Tetracycline, Adsorption, Isotherms, Kinetics, Thermodynamics

CONTENTS

< LIST OF TABLES>

\<LIST OF FIGURES\>

CHAPTER 1

INTRODUCTION

1.1   Water scarcity

The resource of freshwater for human use is immediately decreasing around the world [1]. Forty percent of world population in 80 countries is experiencing depletion of water. From these eighty water-scarcity countries, thirty are enduring from severe water scarcity [2]. The entire renewable water resources of the world are shown in Fig 1.1. Therefore one of the most serious problem of water scarcity, is becoming a threat to global sustainable development [3], due to the increasing population growth from three billion to seven billion people in the last five decades [4]. The increasing world population, improving living standards, changing consumption patterns, and expansion of irrigated agriculture are the main driving forces for the rising global demand for water [5]. Furthermore, water-scarcity areas are experiencing degradation of their water resources both in terms of quality and quantity. The scarcity of water gives in excessive problems such as escalation of famine, poverty, disease within the society, and disturbance in social equilibrium due to intra-country and inter-country migratory fluxes of populations, which occur in search of a better quality of life [6].
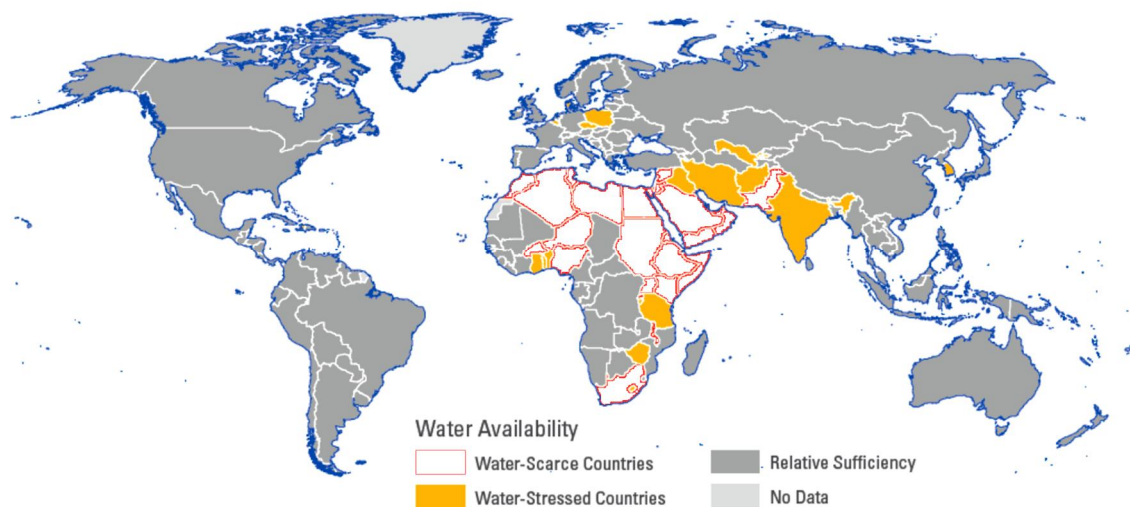
Fig 1.1 Entire renewable water resources in each country from 2008 to 2012 divided by the world population in 2010. [4].

The sustainable use of water implies resource conservation, environmental friendliness, technological appropriateness, economic viability, and social acceptability of development issues. In order to provide safe drinking water and basic sanitation in countries for human, new technology need to be developed and applied to solve these faced problems of water for sustainable solution of wastewater treatment and reuse. There are various contaminants exist in water. The frequent occurrence of pharmaceutical contaminant is one of them.

1.2 Antibiotics in water

Over the last decades, antibiotics are drastically consumed in treating infectious diseases for human and animals [7,8]. Researchers are interested in antibiotic residues of the environment, which is mainly due to their immoderate occurrences and persistent property [8,9]. Also they have noted that concentrations of antibiotics in surface waters, ground water and treated water are 0.1 µg/L and 0.05 µg/L [10]. Antibiotics usually enter the environment either through excretion from human and animals or through the direct disposal of unused or expired medicines in wastewater from hospital, pharmaceutical industry and domestic sewage [11,12]. These can end up in a food chain through bioaccumulation of the aquatic flora and fauna [13]. The fate and pathways of pharmaceuticals in the environment are showed in Fig 1.2 [10,12].
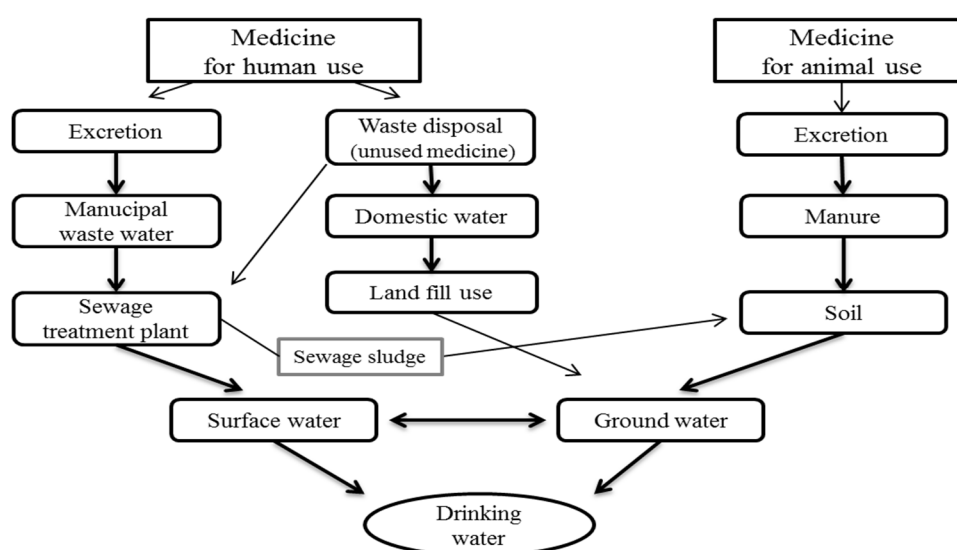
Fig 1.2 Sources and pathways of pharmaceuticals entering the aquatic environment

Tetracycline (TC) is one of the most widely used antibiotics because of its wide spectrum of activity, availability, and recommendation by WHO in "Model List of Essential Medicines" [10,11,14]. TC is used in livestock and poultry breeding to prevent and cure diseases, promote animal growth, and improve food utilization efficiency [15]. It is mostly released by way of urine, feces and manure from human and animals after treat into the environment. Residues of TC are often detected in surface and ground water and soils from agricultural water and waste water treatment plants near to city [16]. The concentrations of tetracycline in the environment such as surface waters are usually 0.11- 4.2 µg/L [8,16], wastewaters are 30.5–388.70 µg/L [15]. Because tetracycline is poorly digested or non-absorbed by the humans and animals, large fractions are excreted through urine and feces as unmodified parent compound [17]. Therefore antibiotics are spread in the environment that can be existed in the food chain by water, vegetables and meat [13]. The excessive and continual use of antibiotics leads to the

weakening of the immune system of the human body. Therefore, it is significant to remove tetracycline from water.

1.3   Water treatment technologies

There are number of methods available to remove antibiotics from contaminated water including advanced oxidation, biological treatment, photo degradation and adsorption. Even though some methods such as advanced oxidation can efficiently remove antibiotics, they are costly and difficult to handle the residues further. Antibiotic removal efficiencies during wastewater and drinking water treatment are dependent on their physical and chemical properties [10].

Oxidation processes are chemical treatment process for removal of organic and sometimes inorganic materials from water and waste water. Strong oxidant contaminants are oxidized to intermediates that are supposed to be less stable and hazardous in the oxidation process [18]. For instance, advanced oxidation process generally involves producing and using free radical, hydroxyl as a strong oxidizer for damaging compounds in which cannot oxidize completely.

Biodegradation is a process using microorganisms to convert and degrade contaminants. This process is widely used treatment method for removal of toxic organic compounds from water and waste water [19]. The process is occurred in an aerobic or anaerobic condition. For example, removal rate of tetracycline by aerobic granular sludge as biological treatment was 81% after 30 days of operation [15]. So, disadvantage of this process is spent long time for treat.

Photo degradation can be important process for removal of organic contaminants depending on the light sensitivity characteristics of the compounds [20]. This process can occur directly or indirectly. In the direct process, contaminants absorb photon which leads to degradation of contaminants to another new product. In an indirect process, absorption of photon by photosensitizers including hydrogen peroxide leads to production of reactive compounds that cause degradation of contaminants. Disadvantage of photochemical process needed high energy consumption and cost of reactors [21].

Adsorption is the mostly used technology for treating water and waste water by removing antibiotics. This process is considered as low cost and simple operation [22,23]. Probably, the one advantage of adsorption is its ability to remove contaminants without separating or transforming them. Adsorption is capable of removing the contaminants from the water without forming hazardous byproducts, whereas chemical treatment can make in the formation of undesirable daughter products. For instance, hydrogen peroxide is used to remove phenols and herbicides by the Fenton process in water [18], but it also reacts with organic compounds and generates harmful compounds [24]. For that reason, chemical treatments sometimes transform the contaminants into daughter compounds, which might be more hazardous than the parent compounds.
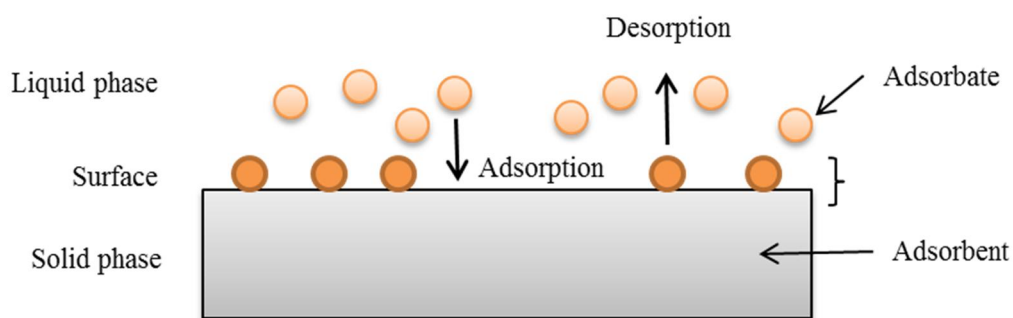
Fig 1.3 Fundamental process of adsorption

Adsorption is a phenomenon in which the particles (contaminants) transfer from liquid phase to attach at the surface of the solid (material). This fundamental process is showed in Fig 1.3 In adsorption processes, the contaminant (molecules) retained on the solid is called adsorbate, whereas the solid is called as an adsorbent [25]. The release of adsorbed molecules back to liquid phase is called desorption. It could be carried out by modifying the temperature, pressure, pH and concentration of the liquid phase. The mechanism of adsorption can be mainly classified into two groups as physical adsorption (Van Der Waals forces) and chemical adsorption (Characteristic of covalent bonding) [26]. The difference of characteristic between physical and chemical adsorption is tabulated in Table 1.1. In physical adsorption, the forces between adsorbate and solid surface are relatively weak, while the forces in chemical adsorption are strong. In chemical adsorption, formation of chemical bonds takes place between adsorbate and solid surface.

Table 1.1 Characteristics of physical and chemical adsorption.

Physical adsorption	Chemical adsorption
Low heat of adsorption	High heat of adsorption
Multi-layered sorptive	Mono-layered sorptive
Reversible	Irreversible
No electron transfer	Electron transfer leading to bond formation between sorbate and solid
Only significant at relatively low temperatures	Possible over a wide range of temperature

Adsorption processes have been used to remove nearly 30 kind of antibiotics with removal efficiencies in the 90-100% at mg/ L concentration levels in the contaminated waters [22]. Various adsorbents have been studied to be effective at removing tetracycline using activated carbon, carbon nano tubes, bentonite and biochar of rice straw [13,22]. Nonetheless, these materials are relatively expensive and lower cost alternatives are desired for large scale water treatment operation [27].

1.4   Using pine bark biochar as adsorbent in water treatment

Adsorption process consists in the transfer of contaminants (Antibiotic) from water to the surface of solid, highly porous material (adsorbent). Adsorbents can be organic or inorganic material. Biochar is an attractive material with important adsorptive properties due to its porosity, high surface area and surface chemistry [28]. Adsorbents developed from raw materials containing lignin and cellulose were effective in the removal of organic compounds [29]. Researchers used various adsorbents for removal of tetracycline from aqueous solution. There are many adsorbents that are used to remove TC from water such as activated carbon, bamboo charcoal, rice husk ash, ferric activated sludge and carbon nano-tubes etc. [17,30,31]. The most common way to carbonize raw material as a biomass is pyrolysis. Pyrolysis is the process of thermal conversion of organic matter using a catalyst in the absence of oxygen [28]. For example, activated carbon is commonly used for cleaning water. But materials for preparation of activated carbon were costly and rare. Therefore, researchers take attention on the finding a way of economically and eco-friendly alternative raw materials to make an activated carbon. Lignin (wood) leads to chars or activated carbon with high porosity and high surface area.

Fig 1.4 Pine trees

In fig 1.4, pine trees are appeared in the small forest. Pine bark, as inexpensive and abundantly available forest waste, can be the possible option for development of bio-adsorbent. Therefore, the pine bark was used for making the biochar. No research has been studied to investigate the capability of adsorbents made of pine bark biochar for removal of antibiotic from water. For adsorption capacity and recovery improvement, the pine bark biochar was modified by iron solutions, which was magnetic and non-toxic. It can easily to separate the biochar particles from the treated water when compare other adsorbents [32]. Magnetic separation has been reported to be one of the good technologies for separating solid and liquid separation because it is more efficient than centrifugation or filtration [33].

1.5   Tetracycline as adsorbate

Tetracycline (TC) is the most commonly used antibiotic around the world with a broad spectrum of activity which can against infections caused by gram positive and gram negative microorganisms [8]. Tetracycline is consumed for medical, veterinary area and agriculture sector due to their lower cost and higher antimicrobial activity [8,11]. The worldwide usage of tetracycline antibiotic for veterinary is shown in Fig 1.5.
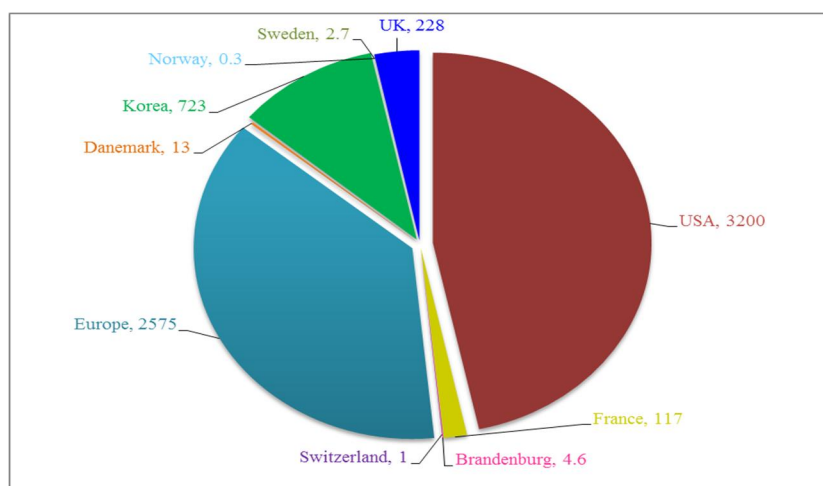
Fig 1.5 The total amounts (unit is tons) of tetracycline antibiotics used for veterinary around the world [8].

TC molecular formula is $C_{22}H_{24}N_2O_8$ and molecular weight is 444.43 g/mol. TC is an amphiprotic compound with multiple functional groups such as amino, phenol and alcohol [11]. TC is identified in the aqueous solution at different pH values. The aqueous dissociation constants are $pK_{a1}=3.3$, $pK_{a2}=7.7$ and $pK_{a3}=9.7$. TC exists in the solution as TCH^{+3} when pH below 3.3, TCH^2 and TCH^- when pH 3.3 to 7. At high pH values 7.7 to 9.7 TC exists as TCH^- and TC^{2-}.
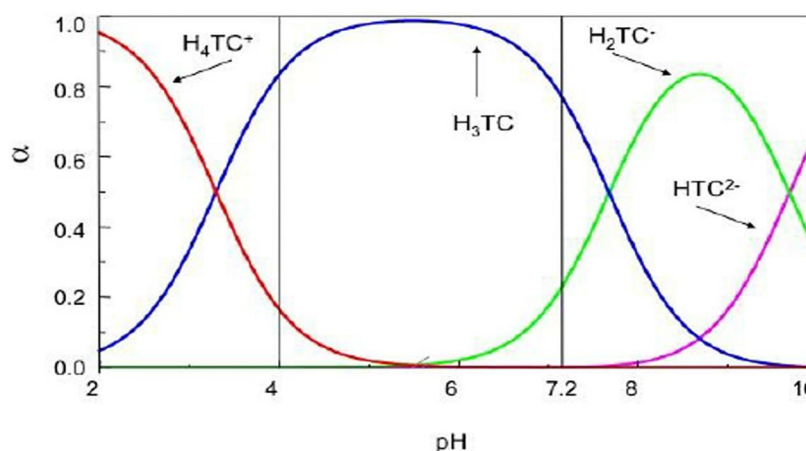
Fig 1.6 Distribution of the different Tetracycline species as a function of pH [34].

1.6   Organization of the dissertation

Chapter 1 provides a general introduction of antibiotics in the aquatic environment, relevant treatment technologies, and significance of adsorption onto magnetic pine bark biochar for antibiotic removal. It also includes organization of dissertation and research objectives and experimental process.

Chapter 2 provides methods of the preparation of pine bark biochar and modification of pine bark biochar by iron solution, and their characterization and effect of factors were analyzed. Also, it includes theory of the isotherm, kinetic models and equipment for characterization.

Chapter 3 presents the results obtained for the removal of tetracycline from aqueous solution. Pine bark biochar and magnetic pine bark biochar were compared with their adsorption capacity for removing tetracycline.

Chapter 4 presents the conclusion of this work.

1.7 Knowledge gaps and Research goals

There can be several ways to remove tetracycline from water such as catalytic degradation, filtration, adsorption, etc. However, some treatments lead to ineffective removal (membrane filtration) or even generation of more harmful products (catalytic degradation). Based on literature review, there is a possibility to develop cost effective and high capacity adsorbent based on pine bark biochar for removal of tetracycline from water via adsorption pathway.

The objective of this research is to evaluate the potentiality of modified biochar from pine bark for removal of emerging contaminant (tetracycline as antibiotic) from water. The determined objective is proposed as follows:

- Development of low costly adsorbents from pine bark through thermal and chemical treatments.
- Characterization studies of PBB and M-PBB
- Investigation of the effect of several factors on the adsorption removal efficiency including the effect of solution chemistry (pH), dosage of adsorbent, contact time, initial concentration and temperature.
- Determination of adsorption isotherms, kinetics and thermodynamics for express the experimental data of TC adsorption by M-PBB. The conceptual diagram of experimental process of adsorption of tetracycline is showed in Fig 1.7.
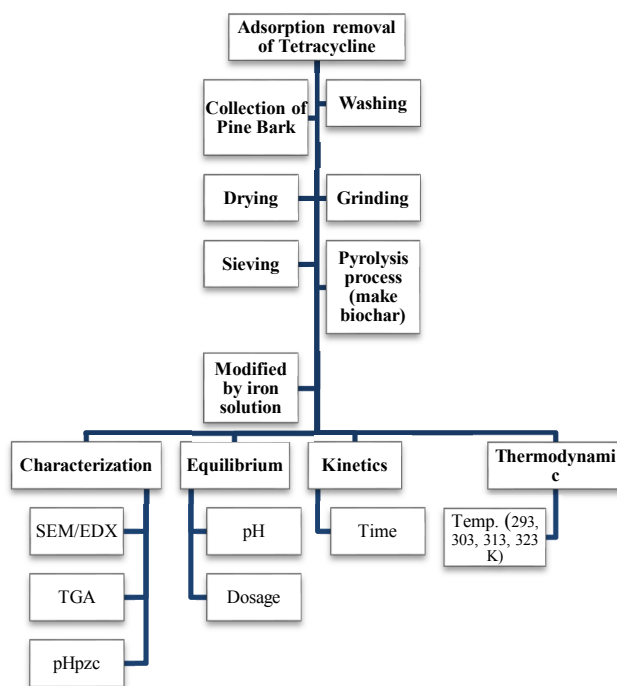
Fig 1.7 The experimental design for adsorption of tetracycline

CHAPTER 2

MATERIALS AND METHODS

2.1   Chemicals for experiment

First of all, reagents used in all experiments were arranged and purchased. $FeSO_4 \cdot 7H_2O$ (purity is higher than 98%) was purchased from Junsei Chemical Co., Ltd., Japan. NaOH (purity is higher than 98%) was acquired from Oriental Chemical Industry, Korea. Tetracycline (purity is higher than 98%) and $FeCl_3 \cdot 6H_2O$ (purity is higher than 98%) were obtained from Sigma-Aldrich, MO., USA. HCl ($\geq$ 36%) was supplied by Daejung Chemicals & Metals Co., Ltd., Korea. Distilled water was used in all experiments.

2.2   Collection of pine bark

Pine bark was collected from ground of under the trees near to UOU for making biochar. The sample was washed with distilled water four times, dried in an oven at 50 $^{\circ}$C for 24 hours. The dried pine barks were milled and sieved with mesh size (100µm). Then the crushed materials were stored in a Ziploc plastic container.

2.3   Preparation of pine bark biochar

The crushed materials were put in clean crucible and carbonized by pyrolysis process in tubular furnace (DTF-40300, Daeheung Company, Korea) for making biochar at 600 $^{\circ}$C with nitrogen flow 1 L/min for 4 hours. After cooling down pine bark biochar were stored in the air tight plastic container for using in experiment. The prepared pine bark biochar was balanced ($\approx$ 25 g) by weighting machine. The procedure of making PBB is presented in Fig 2.1.

Equipment and materials:

- Pine barks
- DI water
- Drying oven
- Milling machine
- Plastic container
- Tube furnace for pyrolysis
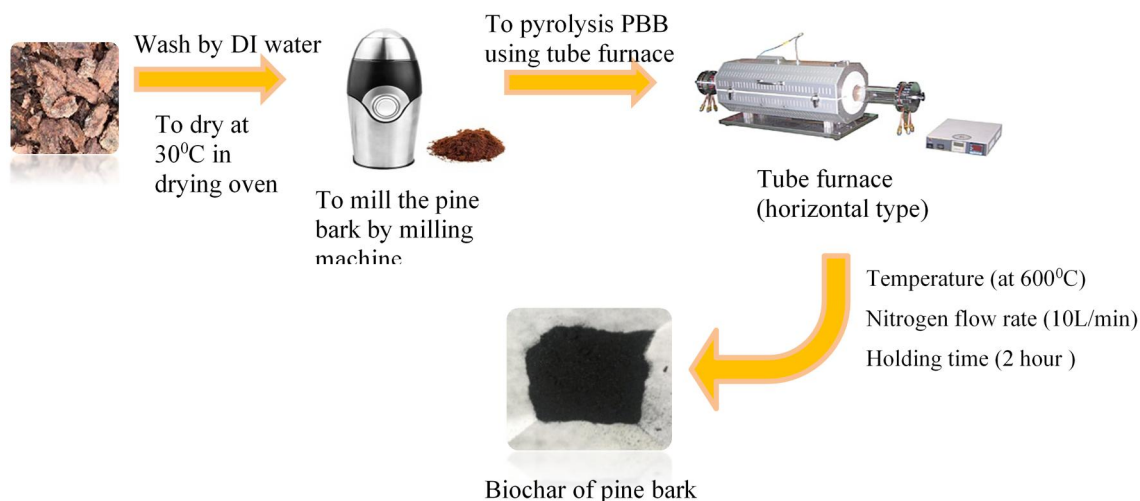
Fig 2.1 The process of making PBB

2.4 Modification of pine bark biochar

The modification of PBB was prepared following steps: (1) The prepared PBB with 10 g was added into a beaker with 100 ml of deionized water. (2) $FeCl_3$ (Iron (III) chloride) and $FeSO_4$ (Iron (II) sulfate) chemicals were added to another beaker with 300ml of deionized water and (3) stirred until they were dissolved completely. Then (4) the previous prepared two solutions were mixed at room temperature for 20 minutes. (5) 5 M concentration of NaOH was added drop wise into the mixed suspension until pH 10-11. (6) The suspension was heated for 1 hour at 90-95 $^{\circ}C$, then (7) it was filtered and washed several times with deionized water. Finally (8) the filtrate was dried at 70 $^{\circ}C$ for 24 hours in an oven. Fig 2.2 is demonstrated general process of modification of M-PBB.
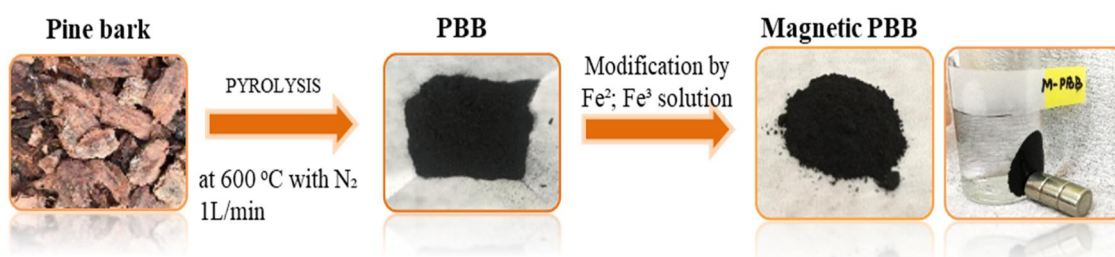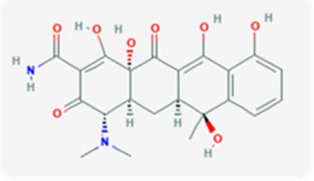
Fig 2.2 Procedure of M-PBB synthesis

2.5 TC solution preparation

Characteristics of the antibiotic are showed in Table 2.1. Distilled water was used for preparing all solutions.

Table 2.1 Properties and characteristic of TC

Chemical structure	Chemical formula	Molecular weight	CAS number	pK$_a$*	logK$_{ow}$*
	$C_{22}H_{24}N_2O_8 \cdot xH_2O$	444.43	60-54-8	3.3 7.7 9.7	-.137

*[22]

In present work, TC stock solution was prepared using distilled water and magnetic stirrer. Predetermined 0.1 g of TC yellow powder were mixed with distilled water in 1L for making 100 mg/L of stock solution and put on the stirrer. Temperature was at (28 °C) and stirring time was 10min until dissolving TC powder. Then prepared TC stock solution was diluted to obtain further desired TC concentration of 25 mg/L (ppm). Although the actual TC concentration in water and waste water is lower than this chosen range, due to limitation of the UV-VIS spectrophotometer (Genesys 10S model, Thermo scientific Co.,). This machine used in present study to detect TC concentrations at 355 nm of wavelength. Also, standard solutions were prepared at different concentration (0.625, 1.25, 2.5, 5, 10, 20, 40, 60, 80, 100 ppm) for knowing limitation of detectable concentration by UV-VIS spectrophotometer at 355 nm. The calibration plot of absorbance versus TC concentrations exhibits a linear relationship between them over the 0.625-10 mg/L (min. concentrations) and 10-100 mg/L (max. concentration). Fig 2.3 is shown calibration curve for detecting concentration of TC.
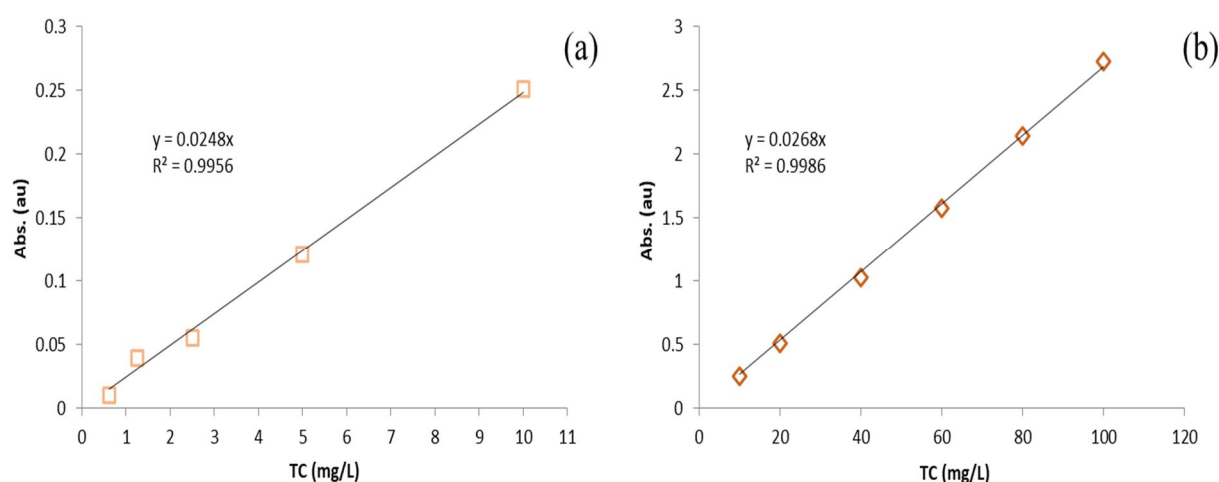
Fig 2.3 Calibration curve for detecting concentration of TC

2.6   Batch adsorption experiments

The adsorption experiments were performed in the batch mode (Fig 2.4). Adsorption studies were performed taking 20 ml of TC solution with 25 mg/L concentration and 0.01-0.2 g (0.5-10 g/L) of PBB or M-PBB into 40 ml vial. The solution pH 2 to 9 value was adjusted using 0.1 M NaOH (Sodium hydroxide) or 0.1 M HCl (Hydrogen chloride). The samples in the vials were sealed and placed in an incubator shaker for shaking at 150 rpm with equilibrated time (16 hours) at room temperature. Then the samples were taken out from the incubator shaker and filtered using filter paper. All experiments were run in duplicate. Residual concentration of TC solution was measured at wave-length (WL) of 355 nm using UV-VIS spectrophotometer (Genesys 10S model, Thermo scientific Co.,).
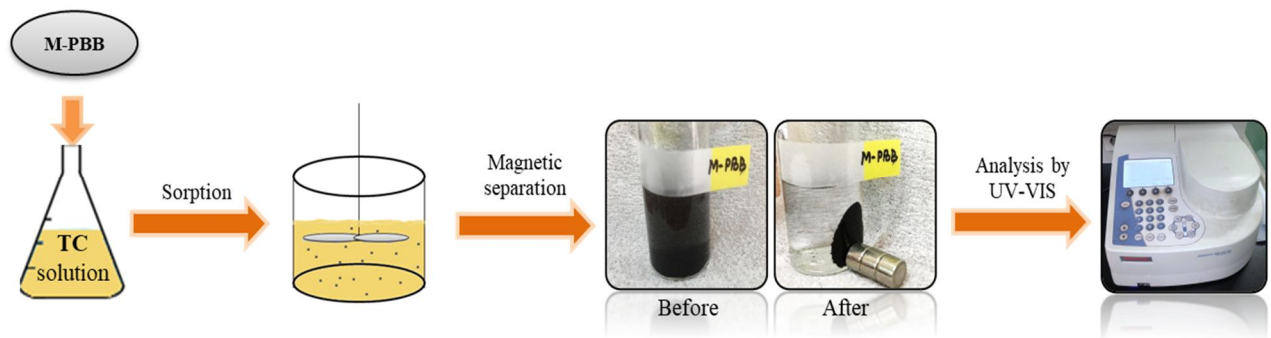
Fig 2.4 Batch adsorption experiment process

2.7   Equilibrium Isotherm and Kinetic studies

The amount of TC absorbed on magnetic pine bark biochar was calculated by the following equation:

$$q_e = \frac{(C_0 - C_e)V}{M} \qquad\qquad (1)$$

Where q_e *(mg/g)* is the equilibrium adsorption capacity, C_0 and C_e (mg/L) are the initial and equilibrium concentrations of TC, V (L) is the volume of solution and M (g) is the mass of biochar.

The kinetic test was performed same as equilibrium test. The prepared samples were taken at different times and the concentration of TC was measured. The equation was written down:

$$q_t = \frac{(C_0 - C_t)V}{M} \qquad\qquad (2)$$

Where, q_t (mg/g) is the amount TC of adsorption at time (t).

2.7.1   Factors affecting adsorption

a.   Effect of pH

The solution pH affects charge state of adsorbent and speciation of adsorbate as well as adsorption process.

Effect of solution pH was observed at pH 2, 3, 4, 5, 6, 7 and 9. Solution's pH was adjusted by 1 M NaOH and 0.1 M HCl. 0.04 g of Pine bark biochar and Magnetic pine bark biochar were added to each 20 mL volume of TC aqueous solution with an initial concentration of 25 mg/L for equilibrium time of 16 hours.

b.   Effect of contact time

Adsorption occurs rapidly because of high concentration of adsorbate leading to existence of stronger mass transfer driving forces at initial stages of contact time. Then adsorption rate decreases constantly when time passes. Finally, the rate of adsorption achieves a steady state which means equilibrium is established between the amount of adsorbate adsorbed and the amount of adsorbate in solution. 0.04 g of Pine bark biochar and Magnetic pine bark biochar were added to each 20 mL volume of TC aqueous solution. The experiments were carried out with the initial concentration of 25 mg/L at room temperature for different times. The times were 0.08 to 16 hours.

c.   Effect of dosage

The effect of adsorbent dosages on adsorption capacity and removal efficiency is evaluated in order to determine the minimum dosage of the biochar needed to reach maximum TC adsorption capacity. So, this experiment was performed as following procedure. Different doses of Magnetic pine bark biochar were added to each 20 mL volume of TC solution. The solution's initial concentration was 25 mg/L and the experiments were carried out at room temperature and at three different pH (3, 6, 9) for 16 hours. The dosages were 0.5, 1, 2, 5, 10 g/L.

The percentage removal of TC was calculated by using the following equation:

$$\% \ Removal \ efficeincy = \frac{C_0 - C_e}{C_e} \times 100 \qquad (3)$$

Where C_o and C_e are the initial and final concentration of TC (mg/L).

d.   Effect of temperature

Temperature can affect equilibrium, kinetic and capacity of adsorption process. Based on the endothermic or exothermic nature of adsorption, temperature effect on adsorption process can explain by an increase of temperature. 0.04 g of Magnetic pine bark biochar was added to each 20 mL volume of TC aqueous solution. The solution's initial concentration was 25 mg/L and the experiments were

carried out at 293, 303, 313 and 323 K for 16 hours. The experiment's temperatures were controlled using incubator with thermostat.

2.7.2 Isotherm models

Adsorption equilibrium will be established between the amount of adsorbate adsorbed and the amount of adsorbate in solution when the adsorbent and adsorbate are contacted for long time [35]. The adsorption performance was represented by Freundlich, Langmuir and Temkin isotherm models. Generally, the mathematical correlation constitutes an important role towards the modeling analysis, operational design and applicable practice of the adsorption systems [36].

a. Freundlich model

This is used most commonly to describe the adsorption characteristics of the activated carbon used in the water and wastewater treatment. The Freundlich model is the empirical adsorption model that can express a quantity of contaminant adsorbed per unit of mass of adsorbent on its surface by multilayer adsorption. The model is commonly used in heterogeneous systems principally for organic or highly interactive compounds on activated carbon [36]. Adsorption intensity or surface heterogeneity is measured by the slope ranges between 0 and 1. If its value becomes closer to 0 surface is more heterogeneous. The parameter n is a dimensionless falling in the rage of 0 to 10. If the value of n higher than 10 an irreversible isotherm is obtained. This model is expressed by the following equation:

$$q_e = K_f C_e^{1/n} \qquad <=> \qquad \log q_e = \log K_f + \frac{1}{n} \log C_e \qquad (4)$$

q_e – mass of adsorbate adsorbed per unit mass of adsorbent (mg/g);

K_f – constant of Freundlich isotherm (mg/g) (L/mg)$^{1/n}$;

C_e – Final concentration of adsorbate (mg/L);

$1/n$ – Freundlich intensity parameter;

b. Langmuir model

The Langmuir model is the most commonly used isotherm for fitting equilibrium data. This empirical model is built based on some assumption. These are: 1) enough number of active sites are on the adsorbent surface by monolayer adsorption (the adsorbed layer is one molecule in thickness), 2) adsorption is reversible. The Langmuir isotherm refers to homogeneous adsorption, which each molecule acquire constant enthalpies and sorption activation energy (once a adsorbate molecule occupies a site)[37]. This model is expressed by the following equation:

$$\frac{C_e}{q_e} = \frac{1}{Q_0 b} + \left(\frac{1}{Q_0}\right) C_e \qquad (5)$$

C_e – Final (equilibrium) concentration of adsorbate (mg/L);

q_e – mass of adsorbate adsorbed per unit mass of adsorbent (mg/g);

Q_0 and b – The Langmuir constants (Adsorption capacity; Rate) (mg/g); (L/mg);

$1/Q_0$ – straight line with slope;

b is expressed as the affinity parameter related to the bonding energy of the adsorbate species to the surface. The essential characteristic of Langmuir isotherm can be evaluated by a dimensionless constant (R_L). It defined as following equation:

$$R_L = \frac{1}{1+bC_0} \qquad (6)$$

b – The Langmuir constant (L/mg);

C_0 – The highest concentration of sorbate (mg/L)

R_L – type of isotherm to be either unfavorable ($R_L > 1$), favorable ($0 < R_L < 1$)

c. Temkin

Temkin isotherm contains a factor that especially taking into the account of adsorbent adsorbate interaction. The model defines adsorption processes occurring on the heterogeneous surfaces based on an assumption. That is heat of adsorption decreases linearly with coverage owing to adsorbate-adsorbent interaction. Temkin model is expressed as following formula:

$$q_e = B \ln K_t + B \ln C_e \qquad (7)$$

C_e – Final (equilibrium) concentration of adsorbate (mg/L);

q_e – mass of adsorbate adsorbed per unit mass of adsorbent (mg/g);

K_t – the maximum binding energy constant (L/mg)

B - the heat of adsorption (mg/g)

d. Dubinin-Radushkevich model (D-R)

The D–R isotherm model describes for the adsorption of adsorbate into the porous structure of the adsorbents. Based on the adsorption potential theory, it assumed that the adsorption process was related to micro-pore volume filling as opposed to layer-by- layer adsorption on pore walls [38]. It also expresses the adsorption mechanism onto a heterogeneous surface. So according to many works of literature, this model's adsorption potential was more expressed as a following equation [36,38]:

$$\varepsilon = RT \ln \left[1 + \frac{1}{C_e}\right] \qquad (8)$$

Where R is the universal gas constant (8.314 J/mol K), T is the absolute temperature (K), and C_e is the equilibrium concentration of adsorbate (mg/L), respectively. This study used linear form of D-R model to fit the experimental data. The linear form of equation is shown in the below:

$$\ln(q_e) = \ln(q_s) - K_{ad}\varepsilon^2 \quad (9)$$

q_e – mass of adsorbate adsorbed per unit mass of adsorbent (mg/g);

q_s- theoretical isotherm saturation capacity (mg/g)

K_{ad} – Dubinin-Radushkevich isotherm constant (mol^2/kJ^2)

ε- Dubinin-Radushkevich isotherm constant

e. Flory-Huggins isotherm model

Flory-Huggins model is the hardly acquiring the degree of surface coverage characteristics of adsorbate onto adsorbent, can express the feasibility and spontaneous nature of an adsorption process. The linear form of model is expressed as following formula:

$$\log\left(\frac{\theta}{C_0}\right) = \log(K_{FH}) + n_{FH}\log(1-\theta) \quad (10)$$

From the equation, θ is the degree of surface coverage, where K_{FH} and n_{FH} are the indication of its equilibrium constant and model exponent. The equilibrium constant is used for the calculation of free Gibbs energy, which is related to the following equation:

$$\Delta G^o = -RT\ln(K_{FH}) \quad (11)$$

All used isotherm models for this study are shown in the Table 2.2. by non-linear and linear form. The linear form of equations are calculated to plot the graphics for explaining the adsorption system.

Table 2.2 Comprising adsorption isotherm models by Non-linear and linear form

Isotherm	Non-linear form	Linear form
Freundlich	$q_e = K_f C_e^{1/n}$	$\log q_e = \log K_f + \dfrac{1}{n}\log C_e$
Langmuir	$q_e = \dfrac{Q_o b C_e}{1 + b C_e}$	$\dfrac{C_e}{q_e} = \dfrac{1}{Q_o b} + \left(\dfrac{1}{Q_0}\right)C_e$
Temkin	$q_e = B\ln K_t C_e$	$q_e = B\ln K_t + B\ln C_e$
Dubinin-Radushkevich	$q_e = (q_s)exp(-k_{ad}\varepsilon^2)$	$\ln(q_e) = \ln(q_s) - k_{ad}\varepsilon^2$
Flory-Huggins	$\dfrac{\theta}{C_0} = K_{FH}(1-\theta)^{nFH}$	$\log\left(\dfrac{\theta}{C_0}\right) = \log(K_{FH}) + n_{FH}\log(1-\theta)$

2.7.3 Kinetic models

Kinetic models have been used to understand the controlling mechanisms of adsorption processes and to predict their behavior over time. The adsorption kinetics was studied through the pseudo first order, pseudo second order, intra-particle diffusion and elovich kinetic modeling. The equations were written as follows:

a. Pseudo first order model

Pseudo first order model determines the rate constant of adsorption. The equation is written as follow:

$$q_t = q_e(1 - \exp(-k_1 t)) \qquad (12)$$

Where, q_e and q_t – the amount of adsorbate adsorbed at equilibrium and at time (mg/g);

k_1 – the rate constant of adsorption (min^{-1})

t – Time (min)

the rate constant of adsorption is determined from the pseudo-first-order expression given by Lagergren:

$$\log (q_e\text{-}q_t) = \log q_e - \left(\frac{k_1}{2.303}\right) t \qquad (13)$$

b. Pseudo second order model

The pseudo-second-order kinetic model is to be successfully applied in the systems where the rate controlling step is chemisorption [39]. This model is expressed by following equation:

$$\frac{t}{q_t} = \frac{1}{k_2 q_e^2} + \left(\frac{1}{q_e}\right) t \qquad (14)$$

Where, q_t and q_e - the amount of TC adsorbed at equilibrium and time (mg/g);

k_2 - the rate constants of the pseudo 2nd order (g/mg h);

c. Intra-particle diffusion model

Intra particle diffusion model can determine the diffusion within the pores is the rate limiting step or not. Generally, for adsorption process to take place adsorbate molecules need to transfer

from bulk phase to the solid surface and then penetrate in the adsorbent pores. The model is expressed by following equation:

$$\text{Intra-particle diffusion:} \qquad q_t = k_i t^{1/2} + C \qquad (15)$$

Where qt is the amount of adsorbate adsorbed at time (mg/g);

K_i is the diffusion rate;

C is value as the constant indicative of boundary layer thickness.

d.   Elovich model

The Elovich equation, which is fitted in chemical adsorption processes and is suitable for systems with heterogeneous adsorbing surfaces [40]. The model can be represented as follow:

$$Q_t = \left(\frac{1}{b}\right) \ln ab + \left(\frac{1}{b}\right) \ln t \qquad (16)$$

$$t_0 = \frac{1}{ab}$$

Where Q_t is the adsorption capacity at time (mg/g);

a is the rate constant of chemisorption;

b is the elovich constant;

t is the time (min);

2.8   Adsorption thermodynamics

Adsorption mechanism and process evaluation of thermodynamic parameter is an important step to determine thermodynamic feasibility. The thermodynamic parameters containing change of standard Gibbs free energy (ΔG^0), entropy (ΔS^0) and enthalpy (ΔH^0) were obtained through thermodynamic functions expressed as follows:

$$\Delta G^0 = \text{-RT ln } K_c \qquad\qquad (17)$$

$$\Delta G^0 = \Delta H^0 - T\Delta S^0 \qquad\qquad (18)$$

$$\ln K = -\frac{\Delta G^0}{RT} = \frac{\Delta S^0}{R} - \frac{\Delta H^0}{RT} \qquad\qquad (19)$$

Where R is the universal gas constant (J/ (mol K));

T is the temperature (K);

K_c is the thermodynamic equilibrium constant;

ΔG^0 is the standard free energy change of adsorption (kJ/mol);

ΔH^0 is the standard enthalpy change (kJ/mol);

ΔS^0 indicates the standard entropy change (J/(mol K));

By (17) equation ΔH^0 and ΔS^0 values can be calculated from the slope and intercept of linear plotting of lnK against 1/T.

2.9   Analytical method

pH is important scale used to specify how acidic or basic a water-based solution. Sample's solution pH value was measured by pH meter (8000 pH meter). TC solution with the biochar was filtered by filter paper. Then, residual concentration of TC solution was analyzed by UV-VIS spectroscopy (Genesys 10S). UV-Vis is simple and inexpensive method to determine the concentration of molecules in solution. These instruments are showed in Fig 2.5.

| **Model:** 8000 pH meter, Eti LTD. | GENESYS™ 10S UV-Vis Spectrophotometer, Thermo scientific. |

Fig 2.5 Instruments for analyses

2.10   Adsorbent characterization

Characterization of PBB and M-PBB were carried out by scanning electron microscopy (SEM), energy-dispersive x-ray spectroscopy (EDX), Differential scanning calorimetry- thermogravimetric analysis (DSG-TGA) and the pH of zero-point charge (pH_{pzc}). These are:

(1) Surface morphology of the PBB and M-PBB were studied using Scanning Electron Microscopy (SEM, JSM-6500F, JEOL) analysis (Fig 2.6). SEM makes images of sample by scanning the surface

with a focused beam of electron. (2) Elemental analysis of PBB and M-PBB were detected by Energy-Dispersive X-ray spectroscopy (EDX, JSM-6500F, JEOL). (3) Weight loss of PBB and M-PBB were studied by DSC-Thermogravimetric analysis (TGA, SDT-Q600). DSC is technique as a thermo analytic in which the difference in the amount of heat required to increase the temperature of a sample and reference is measured as a function of temperature. (4) the pH_{pzc} was analyzed using the method from the literatures. First 1M of stock solutions (HCl, NaOH, NaCl) were prepared and diluted to 0.1M and 0.01M. Concisely, 100 ml of NaCl (0.01M) solution adjusted from pH range of 2 to 10 using HCl or NaOH (0.1M). 10 ml of these pH solutions were placed in 40 ml of vials and 0.05g biochar added to the solutions. Then shake in incubation at 20 $^{\circ}$C and 150rpm for 2 days. The final pH of solutions was measured. The pH_{pzc} from each solution were obtained from the pH (final-initial pH) =0.

| **Model:** SDT (Simultaneous DSC and TGA) Q600 | SEM, JSM-6500F, JEOL |
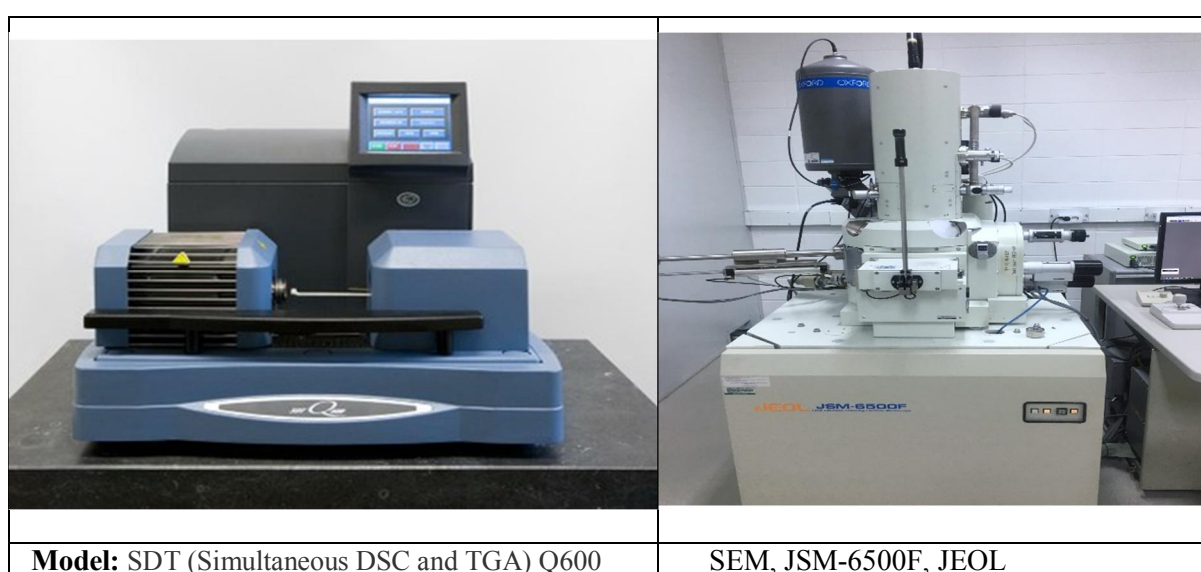
Fig 2.6 Characterizing instruments for adsorbents

2.10.1 Theory of characterization techniques

a. SEM/EDX

Electron microscopy based analysis is very useful in characterizing microparticles, providing information on morphology, size and surface elemental composition. Scanning and transmission electron microscopes are widely used in material science studies [41].

Scanning electron microscope (SEM) is a type of electron microscope that generates high-resolution images of shapes and shows the chemical composition of a sample by scanning it with a focused beam of high-energy electrons. The electrons interact with the atoms in the sample and various signals are generated. These signals are detected by the detectors in the microscope and provide relevant information about the topography and composition of the sample.

The interaction of electrons with matter in electron microscopy can produce different signals which can be used to characterize the sample; secondary electrons to provide information on morphology of the particles, back scattered electrons for detection of high atomic number elements as bright regions and emitted X-rays to provide information on elemental composition. The SEM is also capable of performing analyses of selected point locations on the sample; this approach is especially useful in qualitatively or semi-quantitatively determining chemical compositions analyze combined with Energy Dispersive analysis of X-ray (EDX).

SEM analysis is considered to be "non-destructive"; that is, x-rays generated by electron interactions do not lead to volume loss of the sample, so it is possible to analyze the same materials repeatedly. Essential components of all SEMs include the following in Fig 2.7:

		Electron Source ("Gun")

Electron Source ("Gun")
Electron Lenses
Sample Stage
Detectors for all signals of interest
Display / Data output devices
Infrastructure Requirements:
Power Supply
Vacuum System
Cooling system
Vibration-free floor
Room free of ambient magnetic and electric fields
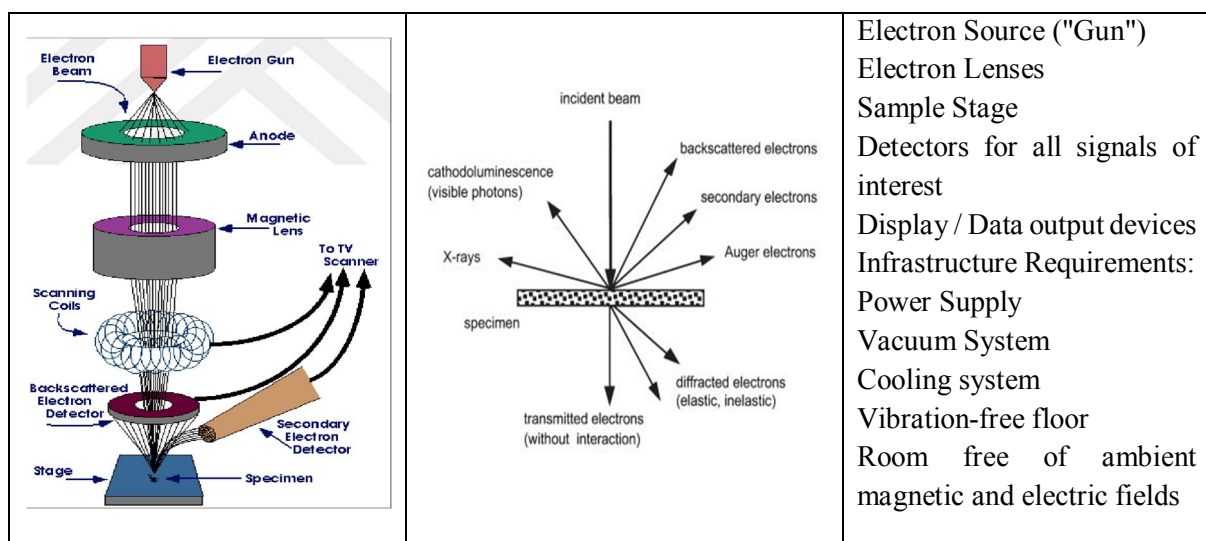
Fig 2.7 Essential components of SEM

Accelerated electrons in an SEM carry significant amounts of kinetic energy, and this energy is dissipated as a variety of signals produced by electron-sample interactions when the incident electrons are decelerated in the solid sample. These signals include secondary electrons (that produce SEM images), backscattered electrons (BSE), diffracted backscattered electrons (EBSD that are used to determine crystal structures and orientations of minerals), photons (characteristic X-rays that are used for elemental analysis and continuum X-rays), visible light (cathodoluminescence-CL), and heat. Secondary electrons and backscattered electrons are commonly used for imaging samples: secondary electrons are most valuable for showing morphology and topography on samples and backscattered electrons are most valuable for illustrating contrasts in composition in multiphase samples (i.e. for rapid phase discrimination).The application of scanning electron microscope combined with Energy Dispersive analysis of X-ray (SEM-EDX) is a powerful technique for the characterization of complex materials.

EDX is a technique that can provide information on the chemical composition of a sample. The technique relies on an interaction of some source of X-ray excitation and a sample. It allows for the identification of particular elements and the relative proportions of a sample. This works best for elements with atomic number (Z) >3. It is generally combined with a scanning electron microscope (SEM) or a transmission electron microscope (TEM). The outputs of EDX analysis normally include a spectrum, map and quantitative analysis of the elements. In the spectrum, peaks reveal the elements that have been identified in the sample. The map provides an image that shows the distribution and concentration of one element within an area of a sample.

b.   Thermogravimetric analysis (TGA)

Thermogravimetric analysis is a method of thermal analysis in which changes in physical and chemical properties of materials are measured as a function of increasing temperature (with constant heating rate), or as a function of time (with constant temperature and/or constant mass loss) [42]. Thermosets generally exhibit mass loss, which provides information about physical phenomena, such as: second-order phase transitions (including vaporization, sublimation, absorption, adsorption, and desorption); chemisorption; desolation (especially dehydration); decomposition; solid-gas reactions (e.g., oxidation or reduction). All of these mass loss processes may be characterized by TGA to yield information such as moisture content, residual solvent, composition, extent of cure and thermal stability. Temperature ranges for commercial TGAs are typically ambient to 1000°C or higher, more than sufficient for thermoset applications. A purge gas flowing through the balance creates an atmosphere that can be inert such as nitrogen or oxidizing such as air or oxygen. Additionally, the moisture content of the purge gas can be controlled anywhere between dry and saturated. Typical sample size ranges from less than a milligram to a gram or more. In Fig 2.8, TGA instrumentation includes furnace, furnace temperature programmer, atmosphere control, temperature sensor, sample holder, recording balance, recorder and balance control. This combination of apparatus allows the sample to be simultaneously weighed and heated or cooled in a controlled manner, and the mass, time, temperature data to be captured. The plot of mass change against time or temperature is called thermogravimetric curve.
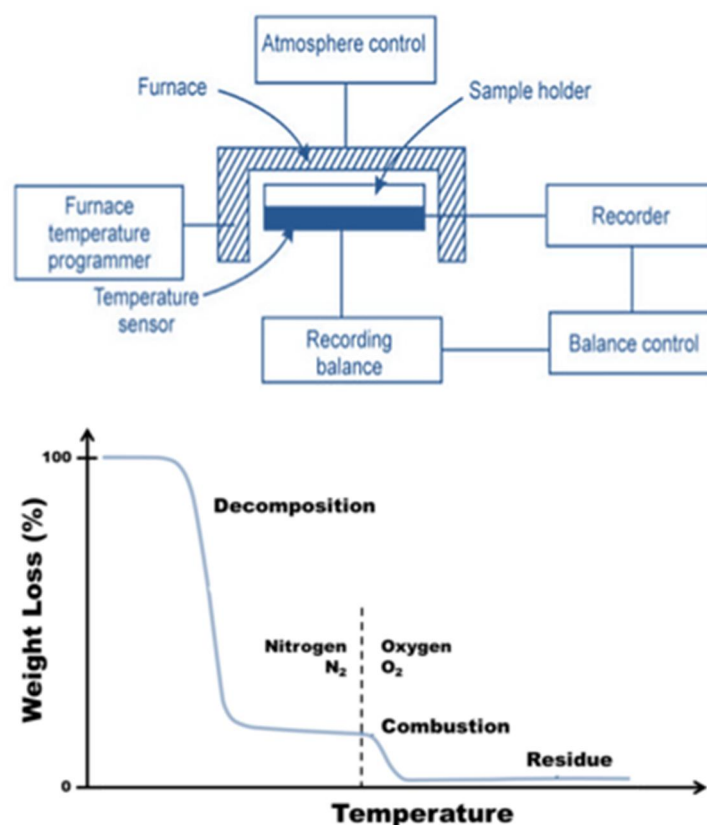
Fig 2.8 Schematic of TGA instrumentation and curve

Differential Scanning Calorimetry (DSC) is used to measure the specific heat capacity of thermally induced events as a function of temperature. Both the sample and reference are maintained at nearly the same temperature throughout the experiment. Generally, the temperature program for a DSC analysis is designed such that the sample holder temperature increases linearly as a function of time. DSC can provide information about physical phenomena, such as: Melting Point/Melting Range; Heat Capacity; Crystallization; Glass Transition; Thermal Stability; Decomposition Temperature; Oxidative Induction Times; Purity [43].

The apparent specific heat (c_2) of a solution is calculated by the following equation:

$$c_2 = c_1 + 1/w_2(c - c_1) \qquad (20)$$

where c is the specific heat of the solution, c_1 is the specific heat of the solvent, and w_2 is the weight fraction of the solute. DSC measures the excess apparent specific heat (c_{ex}), which is the value ($c-c_1$). Expanding the definition of c_{ex} ($c-c_1$), the measured heat capacity of the buffer (c_1) can be written as:

$$C_b = m_b \times C_b^{\circ} \qquad (21)$$

where m_b and C_b° are the mass and the specific heat capacity of the buffer, respectively. Equally, the heat capacity of the sample solution (c) can be expressed as:

23

$$C_s = m_s \times C_s^\circ \qquad (22)$$

with 's' denoting the sample. By subtracting these two values the c_{ex} can be determined. The value (m_b-m_s) can be replaced by the partial specific volume, removing mass from the equation, as new calorimeters use the more precise volume over mass measurements.

The differential heat flow from the calorimeter is temperature dependent and is referred to as a thermo-analytical curve. As the scan rate is constant, the time integral of the measured differential heat flow provides the energy of the sample. As the c_{ex} is usually quite small (about 0.7% for a 1% aqueous protein solution), using equal volumes of solution and proper shielding from external effects is of paramount importance. The excess specific heat is plotted against temperature, revealing the respective transitions. Integration of c_{ex} over the temperature range results in specific calorimetric enthalpy Δh_{cal}. However, traditionally, problems arise when performing integrations. For example, the course of the baseline is not necessarily obvious during a phase transition and may change after the transition, thus, artificial baselines and sophisticated software tools are necessary.

CHAPTER 3

RESEARCH RESULTS AND DISCUSSION

3.1   Adsorbents characterization

In this work, two different materials were used to remove TC from water. First material, pine bark biochar (PBB) was derived from pine bark as forest waste by pyrolysis process. But the adsorption capacity of PBB was not good at adsorbing TC from water. Thus, the biochar was modified by iron solution for enhancing adsorption capacity. This modified biochar (M-PBB) has high adsorption capacity and magnetic (for easily separating adsorbent with contaminant from water) due to iron elements. These materials are showed in the Fig 3.1. In this section, the surface area, surface elements and weight loss of PBB and M-PBB were investigated using SEM/EDX and TGA techniques.

| a. Pine bark biochar | b.   Magnetic pine bark biochar |
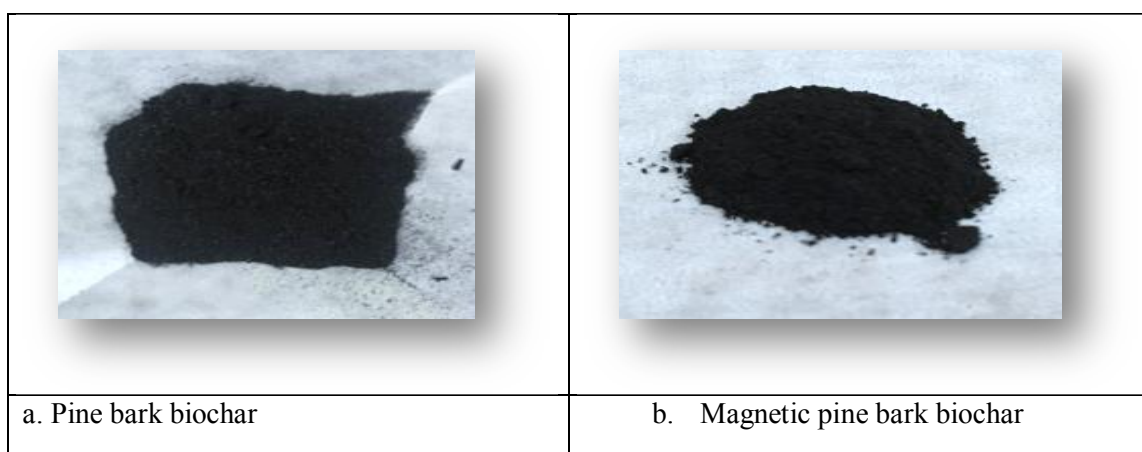
Fig 3.1 Adsorbents (a) PBB, (b) M-PBB

3.1.1   Scanning electron microscopy (SEM)

SEM images of PBB and M-PBB were taken to compare their external morphology. Results of SEM analysis for PBB and M-PBB are shown in Fig 3.2 (a, b). The surface of PBB is revealed smooth in comparison with M-PBB. The M-PBB may become a potentially high adsorption capacity due to roughness surface with iron elements. Then EDX was performed for analyzing the iron element on the surface.

a.	SEM images of PBB

b.	SEM images of M-PBB
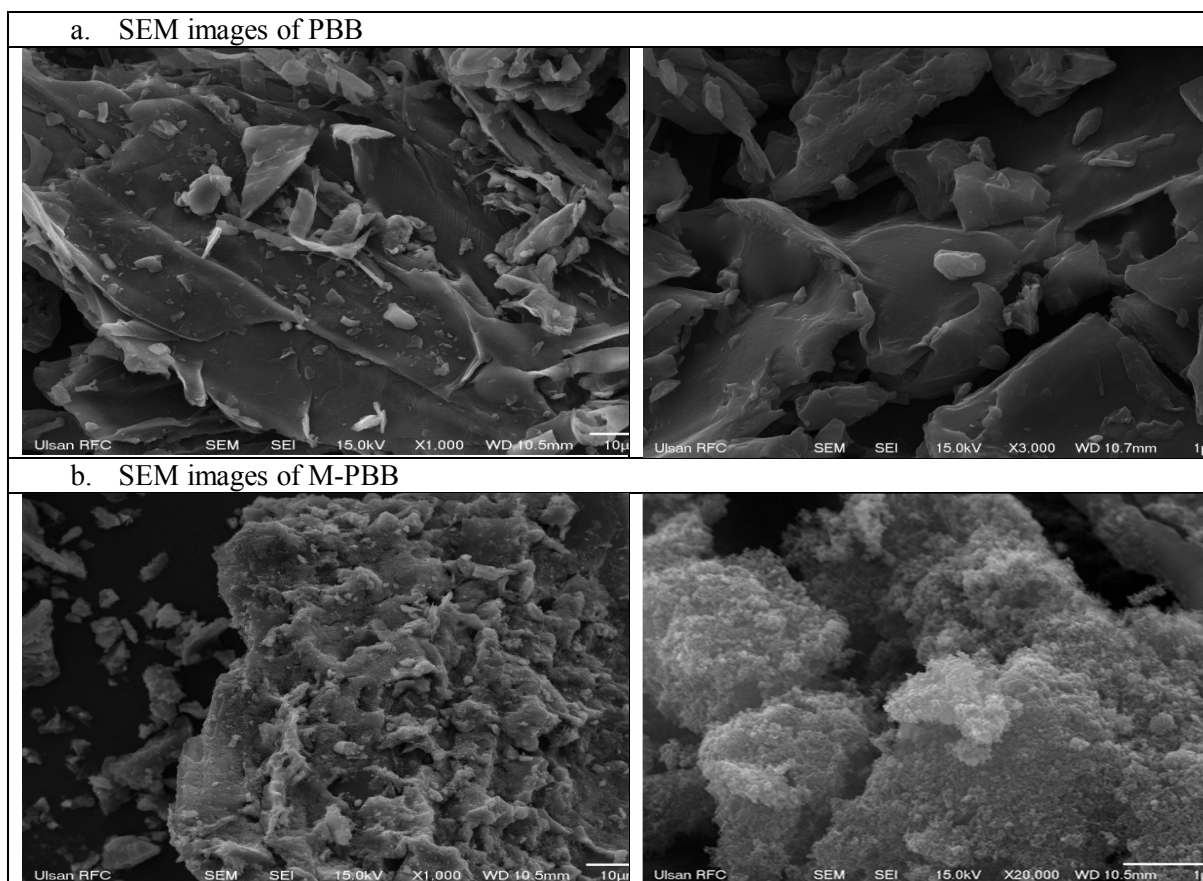
Fig 3.2 SEM images (a) PBB surface, (b) M-PBB surface

3.1.2   Energy-Dispersive X-ray spectroscopy (EDX)

The EDX results shows the identified elements on the surface of PBB and M-PBB in Fig 3.3, respectively. The elements present in the PBB and M-PBB, including C, O, Fe and other small quantity of elements were found by EDX. In Table 4.1, it shows the identified elements on chosen areas of PBB and M-PBB by EDX. Fe compound existed on the M-PBB, and no iron existed in the PBB as control.
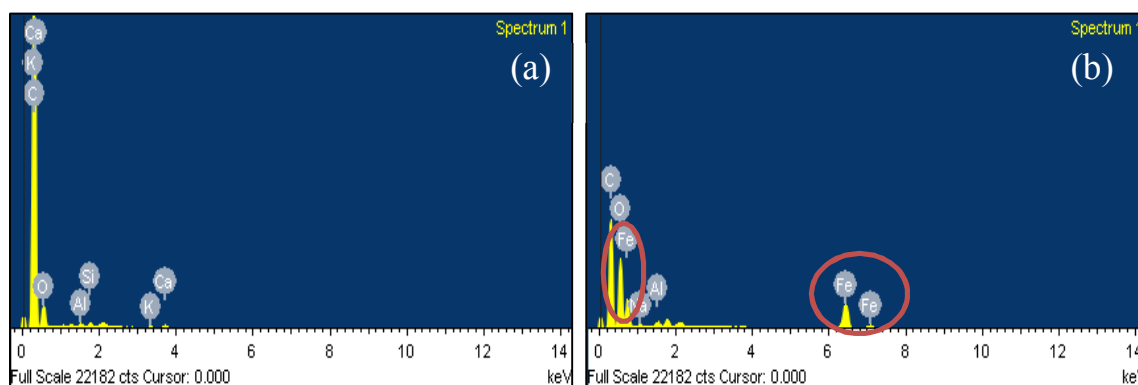
Fig 3.3 EDX results of identified elements a) on PBB surface; b) on M-PBB surface

Table 3.1 Identified elements on the surface of PBB and M-PBB by EDX.

PBB			M-PBB		
Element	Weight%	Atomic%	Element	Weight%	Atomic%
C	89.29	91.93	C	50.86	63.52
O	10.19	7.88	O	34.48	32.33
Ca	0.22	0.07	Fe	14.02	3.76
Si	0.15	0.07	Al	0.33	0.19
Al	0.09	0.04	Na	0.3	0.2

3.1.3 DSC-Thermogravimetric analysis (DSC-TGA)

In order to study the thermal behavior of PBB and M-PBB, analysis was conducted on the two solid samples in a flowing air atmosphere. The TGA results show in Fig 3.4, PBB and M-PBB decomposed approximately at 360°C temperature. Residue of PBB (9.062%) was 4 times lower than M-PBB (36.03%) due to modifying the biochar by Fe. Also, the DSC results are showed in this figure. The DSC heat flow values of PBB and M-PBB were positive when temperature was between 298.9-508°C (PBB), 315-498°C (M-PBB), it illustrated the exothermic reaction. The DSC values of PBB and M-PBB decreased to negative at higher temperature (above 500°C), indicating a shift from exothermic to endothermic reactions.
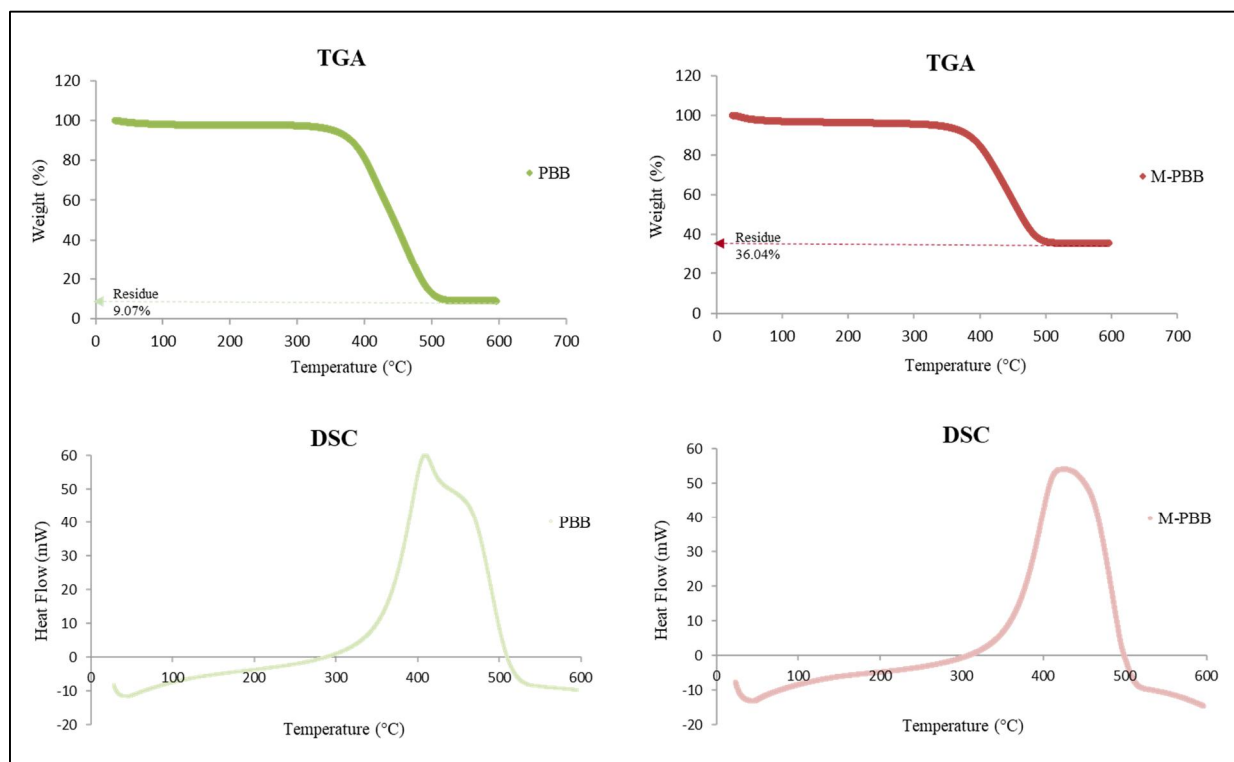
Fig 3.4 TGA-DSG images of PBB and M-PBB

3.1.4 The point of zero charges (pH$_{pzc}$)

The pH$_{pzc}$ of PBB and M-PBB were determined which values were 7.5 and 7.24 (Fig 3.5). The surface charges of these adsorbents were positively charged when the pH was lower than their pHpzc point (pH<pH$_{pzc}$), on the other hand when pH was higher than their pH$_{pzc}$ it was negatively charged(pH>pH$_{pzc}$).
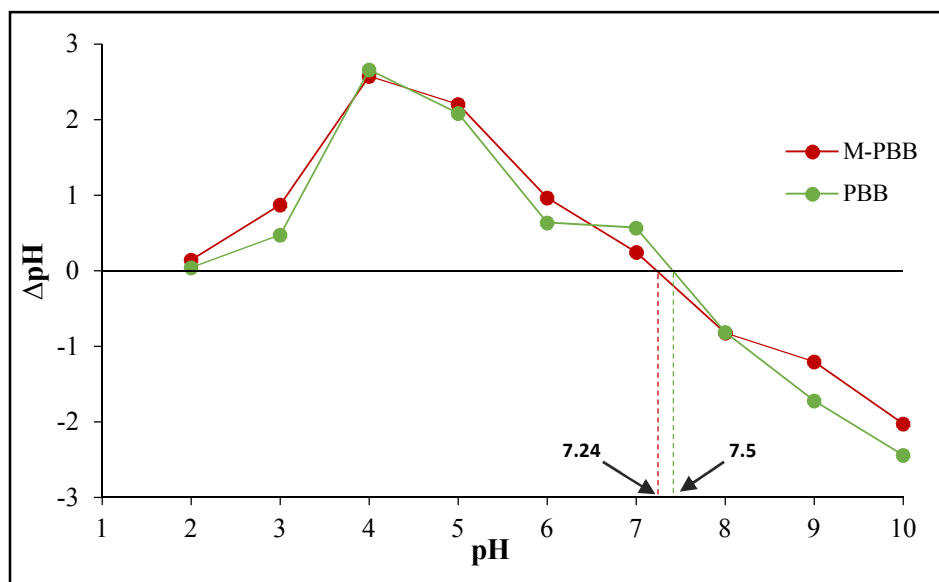
Fig 3.5 Determination of point of zero charge for PBB and M-PBB.

3.2 Adsorption equilibrium (batch experiment)

Effect of pH and contact time parameters on adsorption of TC on PBB and M-PBB was carried out. After these parameter's results were showed PBB adsorption capacity was lower than M-PBB. Therefore, effect of dosage and temperature parameters on adsorption of TC on M-PBB was investigated.

3.2.1 Factors for affecting adsorption

a. Effect of pH

The pH is the important factor in the adsorption process which can effect on adsorption capacity because it changes the surface charge of adsorbent and species of adsorbate [39]. The effect of pH on TC adsorption using PBB and M-PBB was studied in the pH range of 2 to 7. The solution pH was adjusted by 1 M NaOH and 0.1 M HCl. The results are shown in Fig 3.6. Lower adsorption capacity

obtained at pH 2 on PBB ($q_e \approx 2 = 1.77$ mg/g) and M-PBB ($q_e \approx 2$ mg/g). The adsorption capacity (q_e) values increased with increasing pH from 2 to 5. The adsorption capacity was relatively constant in the pH range of 4-5 on PBB ($q_e \approx 2 = 1.97$ mg/g) and M-PBB ($q_e \approx 10.7$ mg/g). The decrease in TC adsorption capacity from pH 6 was appeared. The pH can influence adsorption TC on the biochar by changing properties of the TC and adsorbents. TC is an amphiprotic compound with multiple functional groups such as amino, phenol and alcohol[11]. TC is identified in the aqueous solution at different pH values. The aqueous dissociation constants are $pK_{a1} = 3.3$, $pK_{a2} = 7.7$ and $pK_{a3} = 9.7$ (Table 1). TC exists in the solution as H_4TC^+ when pH below 3.4, H_3TC when pH 3.4 to 7.6 At high pH values 7.6 to 9.7 TC exists as H_2TC^- and HTC^{2-}[39,44]. Effect of pH result on TC adsorption by PBB and M-PBB is explained by interaction between surface charge of adsorbent and TC species. The pH range 2-3.4 was not favorable for adsorbing TC onto the adsorbents due to electrostatic repulsion between H_4TC^+ species and positively charged surface of adsorbent. from pH 3.4 to 7, there is a no electrostatic repulsion occurred due to TC molecules exist no net electrical charge H_3TC species and positively charged surface of adsorbent. Identical trends were showed in previously studied literatures [39,44] for effect of pH on adsorption TC capacity by different biochars. Based on our propose of the study as removing TC from water, further experiments were carried out at pH 6.

Fig 3.6 Effect of pH on TC adsorption capacity of PBB and M-PBB (Initial TC concentration 25mg/L; Dosage 2 g/L; at room temperature; time =16 hrs)

b. Effect of contact time

The effect of contact time on TC adsorption capacity of PBB and M-PBB were studied at different times (5 min to 40 hrs). Fig 3.7. show the amount of adsorption capacity versus the adsorption time at 25 mg/L TC concentration and 2 g/L dose at room temperature. The amount of TC adsorbed increased with increase in time and then reached equilibrium. When time was increased, TC adsorption

capacities (q_t) were increased from 0.7 to 2.5 mg/g on PBB and 6 to 10.3 mg/g on M-PBB. The equilibrium TC adsorption capacities of PBB and M-PBB were achieved in 16 hrs. Therefore, 16 hours was set as the contact time for further studies.

Fig 3.7 Effect of contact time on TC adsorption capacity of PBB and M-PBB (Initial TC concentration 25mg/L; Dosage 2 g/L; at room temperature)

c. **Effect of dosage**

Firstly, the effect of dosage of M-PBB on the TC removal from water was studied. The determination of M-PBB dosage is important because it determines the efficiency of TC removal and may also be used to predict the cost of the biochar per unit of solution to be treated. TC adsorption capacity of PBB from water was lower than M-PBB. This equilibrium experiment was carried out on M-PBB at 16 hours. The effect of adsorbent dose of M-PBB on the adsorption capacity was evaluated at three different pH (3, 6, 9) in order to determine the minimum dosage of M-PBB. As expected, the removal efficiency of TC increases significantly as adsorbent dosage increases. The effect of dosage of M-PBB on the percentage removal of TC is shown in Fig 3.8. The results showed that the maximum TC adsorption capacities were achieved at the dosage of 0.5 g/L ($q_m \approx$ 15.3 mg/g) at pH 6 in a Fig 3.9. Also, the maximum TC adsorption capacities were 10.8 mg/g at pH 3 and 9. Nevertheless 2 g/L of the dosage was chosen for further experiments. In this figure, adsorption capacity decreased with increase in adsorbent doses. Because adsorbent active sites were enhanced.
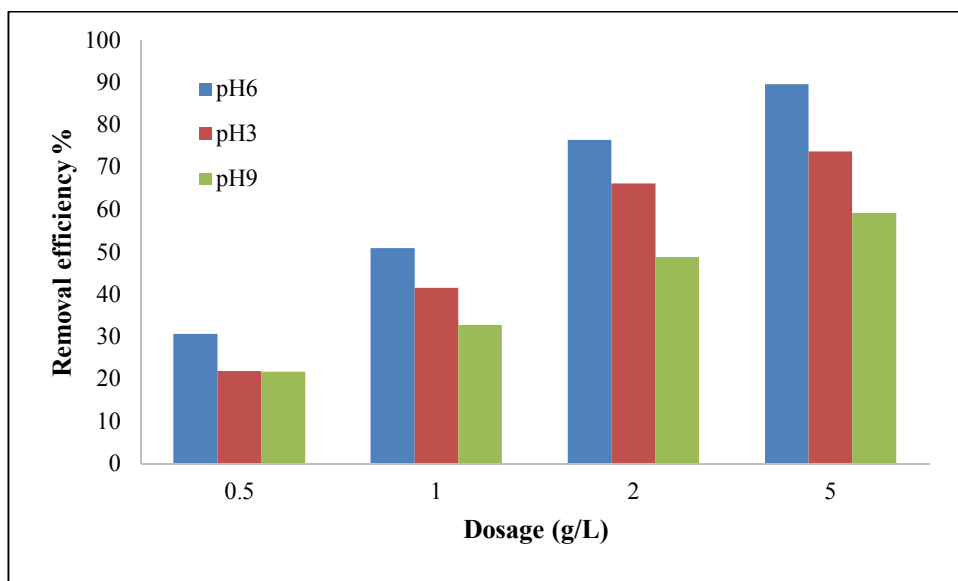
Fig 3.8 Effect of dosage of M-PBB on the removal efficiency of TC (Initial TC concentration 25 mg/L; Dosage 0.5-10 g/L; at room temperature; 16 hrs)
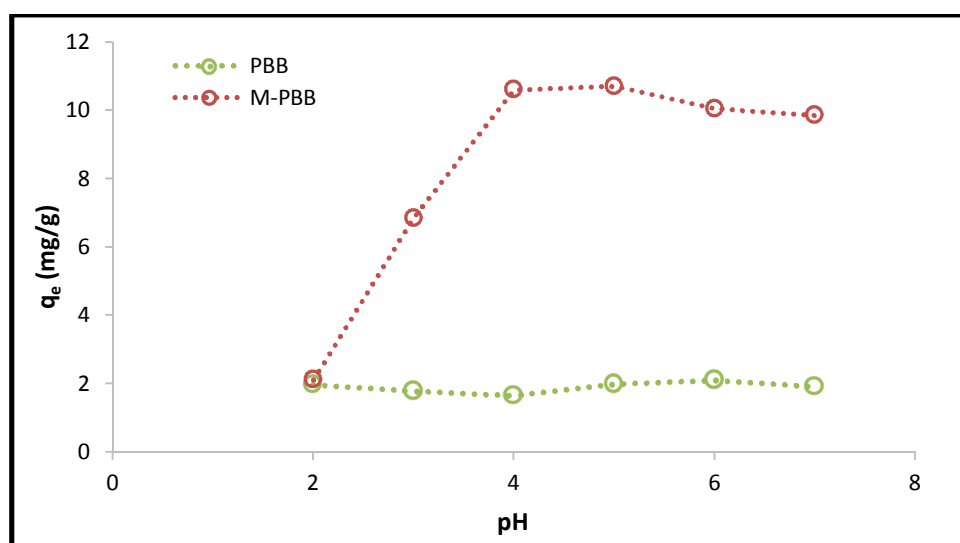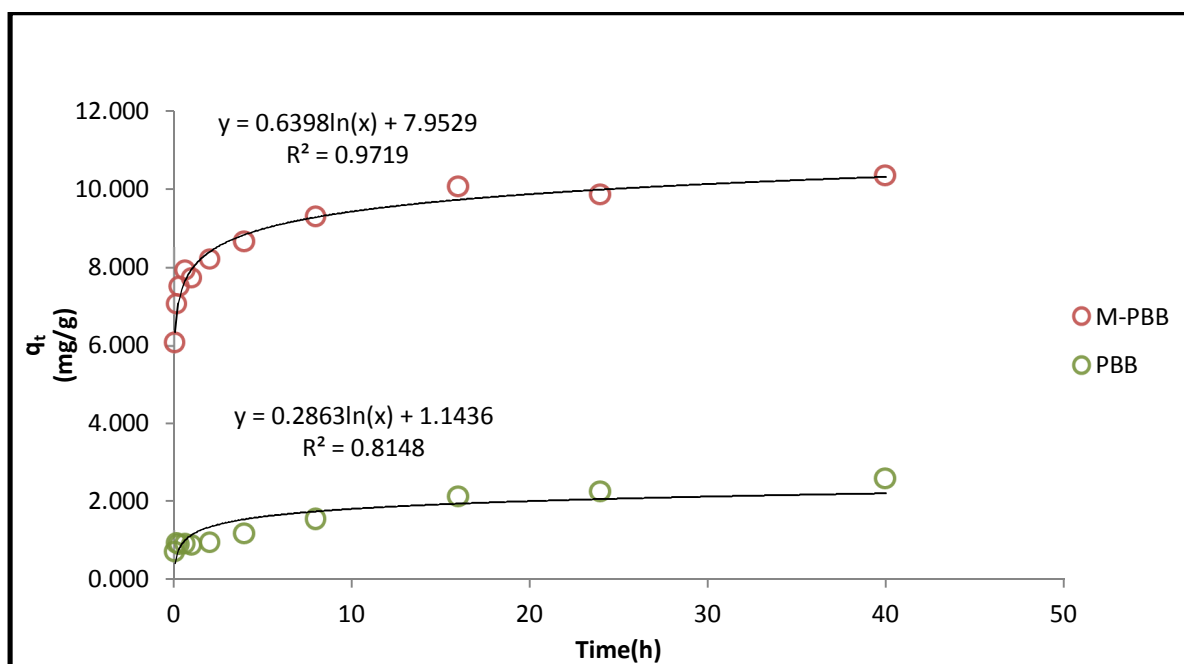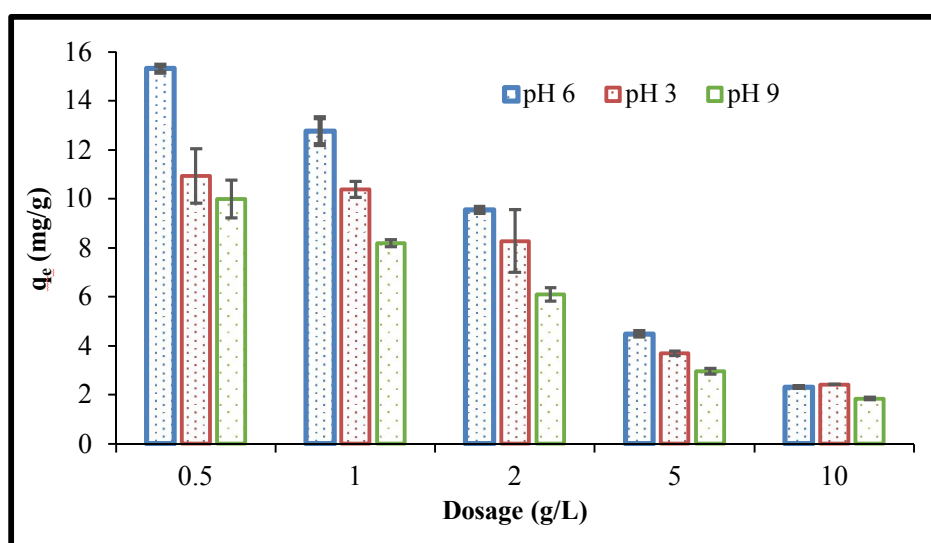

Fig 3.9 Effect of dosage on TC adsorption capacity of M-PBB (Initial TC concentration 25 mg/L; Dosage 0.5-10 g/L; at room temperature; 16 hrs)

d. Effect of temperature

The effect of temperature of M-PBB on the adsorption capacity was evaluated at four different temperatures (20, 30, 40, 50 C$^{\circ}$). The temperature of 30 was chosen to perform for the experiments as the room temperature in summer. This graphic illustrated in Fig 3.10. The TC adsorption capacities of M-PBB were increased as the temperature was increased, which revealed that the adsorption of TC on M-PBB was an endothermic process. The adsorption capacity of M-PBB found to be 9.9, 10, 10.7, 11 mg/g at 20, 30, 40, 50 C$^{\circ}$.
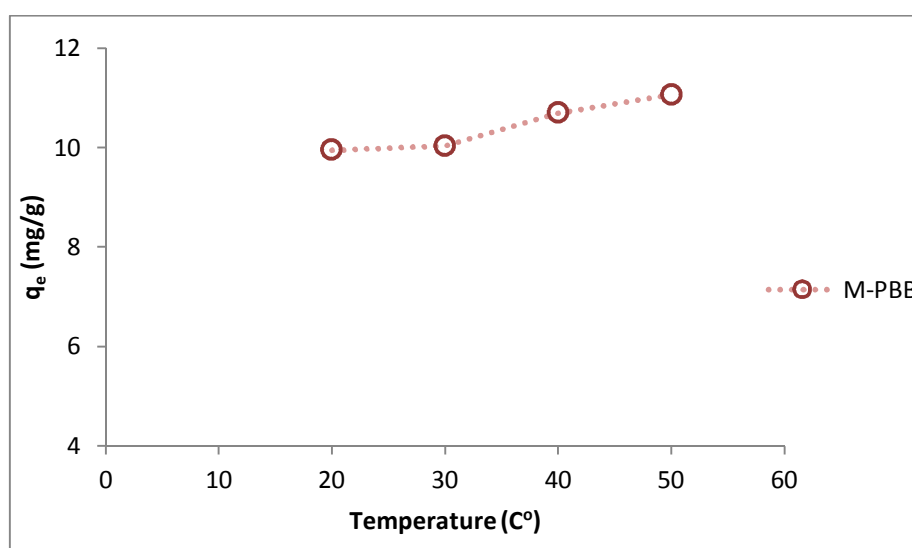
Fig 3.10 Effect of temperature on TC adsorption capacity of M-PBB (Initial TC concentration 25mg/L; Dosage 2 g/L; 16 hrs)

3.2.2   Isotherm modeling

Batch experiments on effect of dosage were conducted at three different pH of 3, 6, 9 at the room temperature. After found TC adsorption capacities of M-PBB, the Freundlich, Langmuir, Temkin and Dubinin-Radushkevich (D-R) isotherms were used to model the experimental data.

a.   Freundlich

The Freundlich isotherm is made by the (3) equation. The plot of Log qe against Log Ce gives straight lines with slope 1/n in Fig 3.11. This figure shows that adsorption of TC follows the Freundlich model according to Freundlich constants (K_F, n) and R^2 value. The values of K_F which is an indication of adsorption capacity has increased at lower and neutral pH conditions. R^2 values were 0.828, 0.936, 0.970 at pH 3, 6, 9. The adsorption of TC on M-PBB follows the Freundlich isotherm in Fig.3.11. This isotherm's parameters were calculated in Table 5.3.
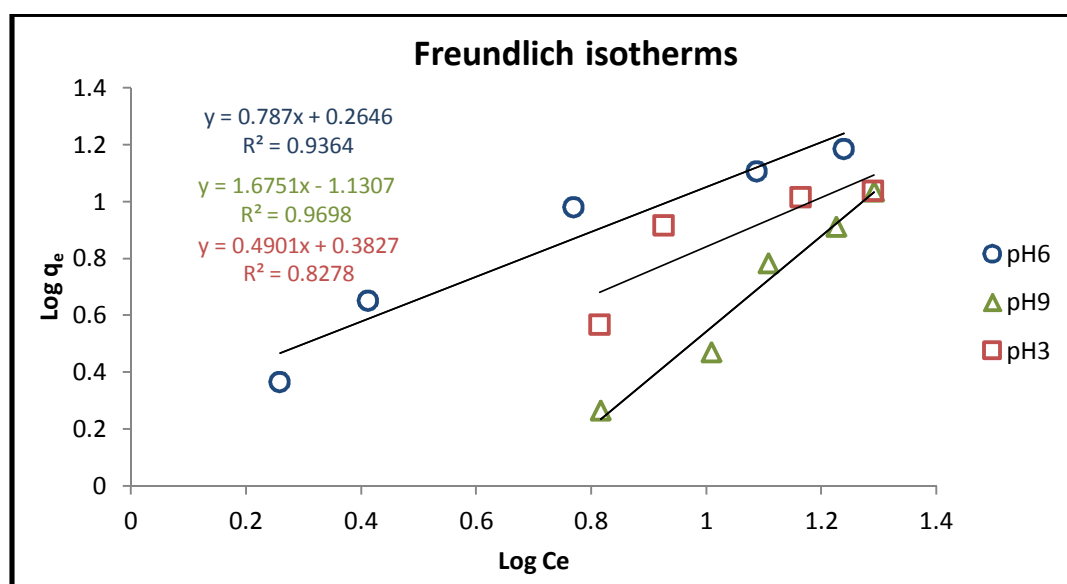
Fig 3.11 Adsorption isotherm of TC on M-PBB by fitting the Freundlich model.

b.   Langmuir

The Langmuir isotherm is built by the (4) equation. Ce/qe was plotted versus Ce gives straight line with slope 1/Qo in Fig 3.12. Langmuir model is not fitted well to explain experimental data. The isotherm constants b and Qo were calculated and their values were shown in Table 5.3. Values of R_L (it indicates unfavorable or favorable) were calculated to be 0.302, 0.423, 5.377 at pH 3, 6, 9. The M-PBB is favorable for adsorption of TC at studied pH except to pH 9. But R^2 values were not close to 0.9 that means Langmuir isotherm was not fit with experimental data.
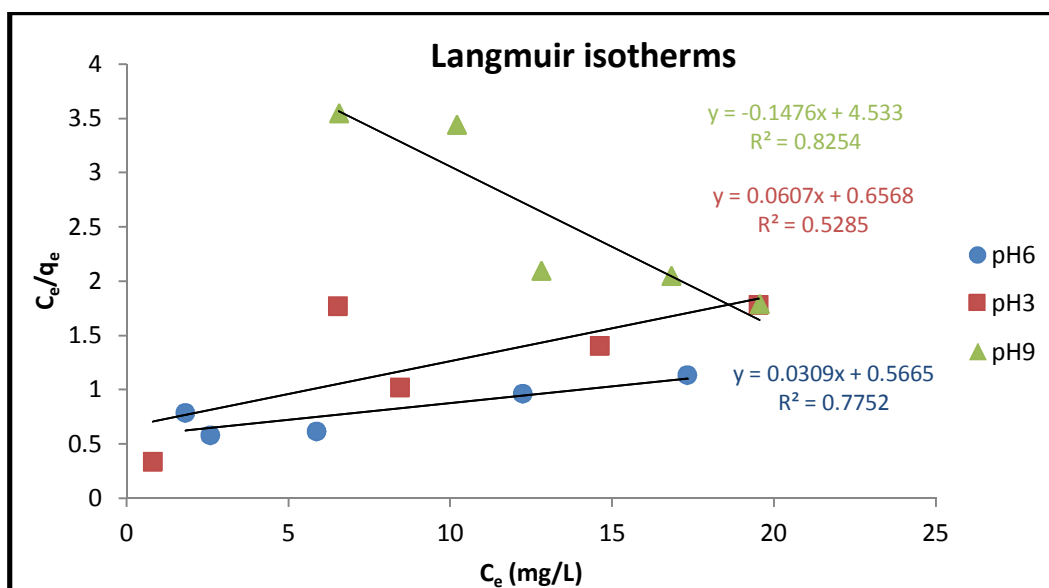
Fig 3.12 Langmuir isotherms for adsorption of TC on M-PBB at different pH.

c. Temkin

Temkin considers heat of adsorption of adsorbate decreases linearly with adsorbent by adsorbent- adsorbate interaction. The Temkin isotherm is built by the (6) equation as shown in Fig 3.13. A plot of qe versus ln Ce can give to find Temkin isotherm' constants of K_t and B. The isotherm showed high R value ($\approx$0.99) at pH 6 in compared with R values of pH 3, 6 ($\approx$0.75; 0.92). The values of parameters shown in Table 3.2.
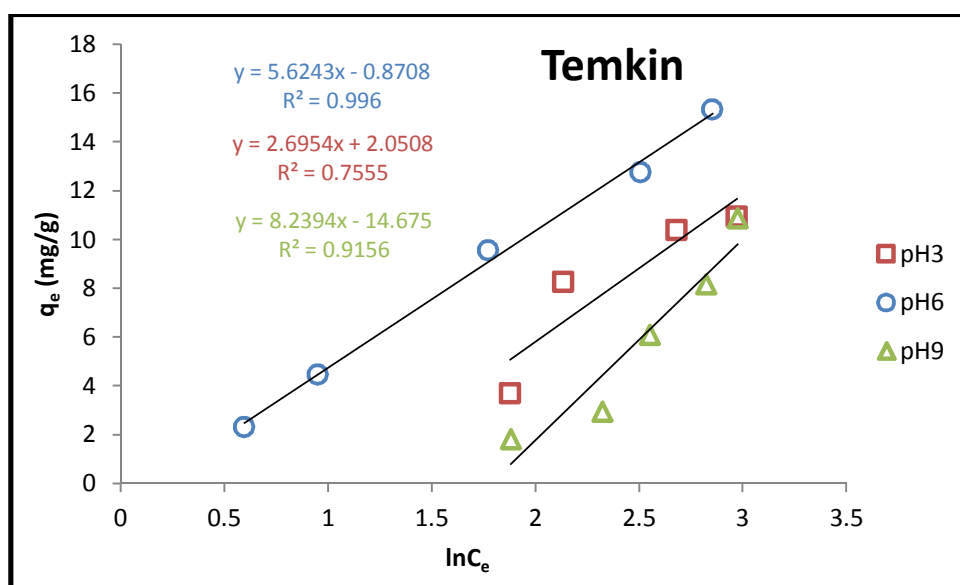
Fig 3.13 Temkin isotherms for adsorption of TC on M-PBB at different pH.

d. Dubinin-Radushkevich (D-R)

D-R model is commonly used to determine the adsorption mechanism onto a heterogeneous surface by Gaussian energy distribution. The isotherm is calculated by (8) equation. The constants of D-R model are obtained from the slope and intercept of the line by fitting lnq_s and ε^2. The values of q_s which is theoretical isotherm saturation capacities were found (7.85, 13.5, 10.6 mg/g) at pH 3, 6 and 9. R^2 values were 0.607, 0.980, 0.861 at pH 3, 6, 9. The adsorption of TC on M-PBB follows the D-R in Fig.3.14. This isotherm's parameters were calculated in Table 3.2. From D-R model, the energy of adsorption (E (kJ/mol)) is calculated to use as following equation.

$$E = (2 \times K_{ad})^{-1/2} \qquad (23)$$

The energy E decreases with pH range 3 to 9 (0.863; 0.167; 0.017 kJ/mol). It indicates that the adsorption mechanism is physical (physical forces like Van der Waals and hydrogen bonds) due to E is lower than 8 kJ/mol [45].
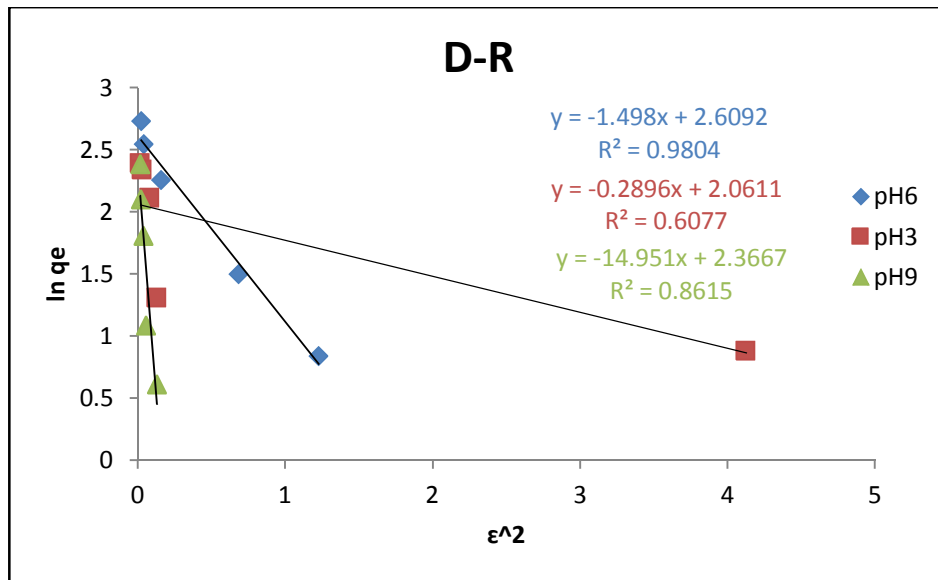
Fig 3.14 D-R isotherm for adsorption of TC on M-PBB at different pH.

Studied isotherm parameters are showed in Table 3.2. Summarizing isotherm studies on adsorption TC from water using M-PBB, the Freundlich model is suggested to be the best fit to express experimental data. Based on the n values derived from M-PBB at pH 3,6,9, the adsorption of TC was favorable (if n values within the range 1-10) [46]. This indicates adsorption of TC to occur on heterogeneous sites on the surface of M-PBB. From Langmuir isotherm, maximum adsorption capacity (Q_0) was 32.3 mg/g at pH 6 comparing with pH 3, 9. But Q_0 is not close to experimental adsorption capacity, so Langmuir isotherm cannot describe the mechanism of TC adsorption by M-PBB. Unlike

M-PBB at pH 3,9, D-R model showed the best fit to the data from adsorption isotherm using M-PBB at pH 6. R value was 0.9804 and q_s was 13.5 mg/g.

Table 3.2 Isotherm parameters for removal of TC by M-PBB at different pH

pH	Langmuir			Freundlich			
	Q_0 (mg/g)	b (L/mg)	R²	n	1/n	K_F (mg/g) (L/g)^n	R²
3	16.474	0.092	0.529	2.040	0.490	2.414	0.828
6	32.362	0.055	0.775	1.271	0.786	1.839	0.936
9	-6.775	-0.033	0.825	0.597	1.675	0.074	0.970

pH	Temkin			D-R		
	B	K_t (L/mg)	R²	q_s (mg/g)	E (kJ/mol)	R²
3	2.6954	2.140	0.7555	7.855	0.863	0.6077
6	5.6243	0.856	0.996	13.588	0.167	0.9804
9	8.2394	0.168	0.9156	10.662	0.017	0.8615

3.2.3 Kinetic modeling

Earlier various kinetic models have been used to know the mechanism of adsorption process and try to explain their attitude over time. Because different kinetic data were obtained at initial concentration (C_0=25ppm) with pH 6 at room temperature. After batch experiment on effect of contact time using PBB and M-PBB, Pseudo first and second order, intra particle diffusion and Elovich models were used to model the experimental data. The determined parameters and correlation coefficients corresponding to the kinetic models applied for expressing experimental data are calculated in Table 3.3.

a. Pseudo first model

From pseudo-first-order expression, values of k_1 and q_e were calculated from the plots of log(q_e-q_t) against t for two materials. It is shown in Fig 3.15. PBB and M-PBB data were not fitted with pseudo first order. So, the correlation coefficient of this model was not good on PBB and M-PBB (R^2=0.35; 0.66). The kinetic data were further modeled using the pseudo-second-order.
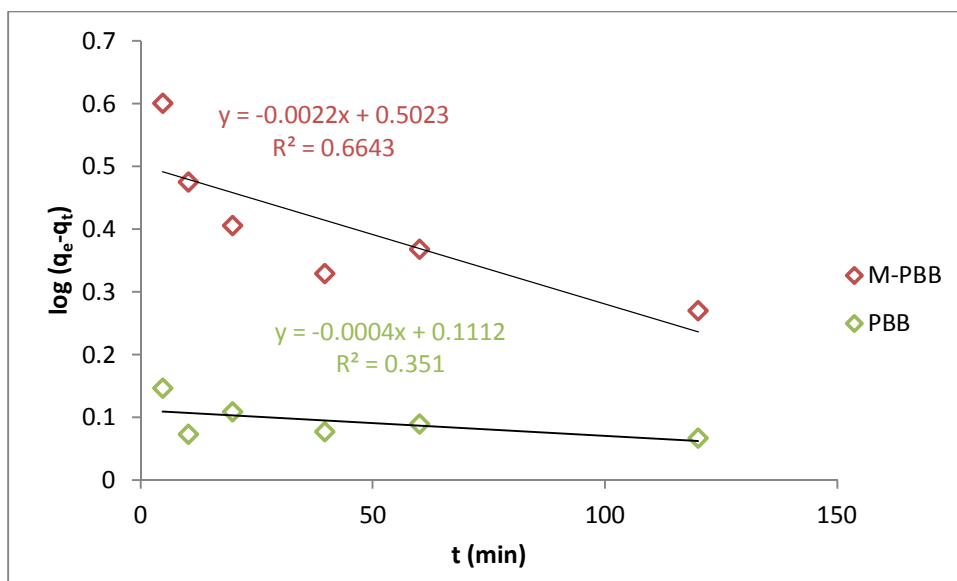
Fig 3.15 Pseudo-first-order kinetics for adsorption of TC on PBB and M-PBB.

b. Pseudo second model

The equilibrium adsorption capacity (q_e) and the pseudo-second-order constant k_2 can be calculated from the slope and intercept of plot t/q_t versus t. It is shown in Fig 3.16. Pseudo second order was the commonly fitted model for TC adsorption on raw and modified biochar [47], based on recent literature. So, in this study, the model fits the kinetic experimental data very well with the correlation coefficient ($R^2 \geq 0.99$) which is better than pseudo-first-order. Pseudo second order was suitable to described the interaction between TC and the biochar (PBB, M-PBB) due to relatively high R^2 value, which indicates chemi-sorptive interaction. Moreover, the equilibrium adsorption capacity (q_e) obtained from the experimental data was closely identical to those calculated (q_e in Table 3.3) from the pseudo-second-order model fitting data.
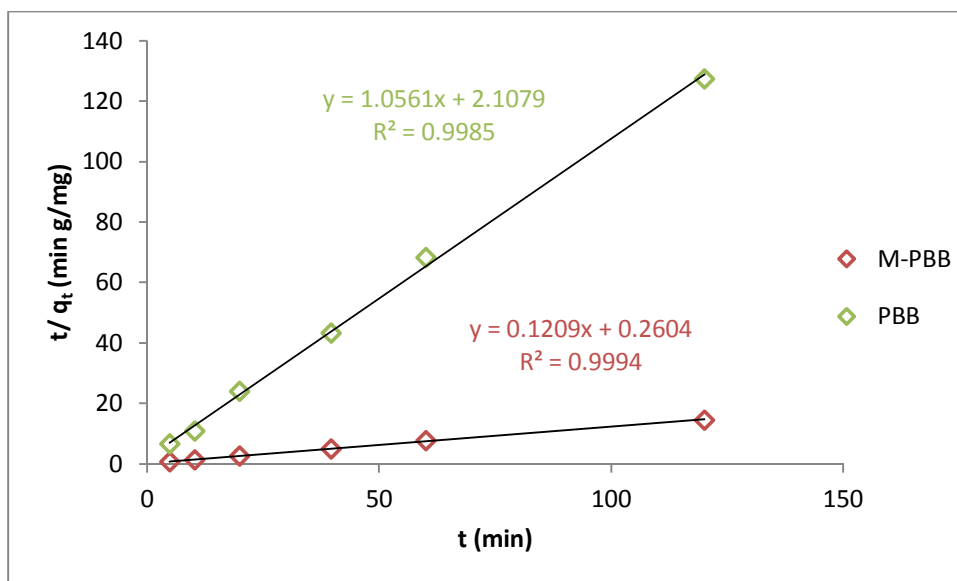
Fig 3.16 Pseudo-second-order kinetics for adsorption of TC on PBB and M-PBB.

c. Intra-particle diffusion

The intra-particle diffusion model's plot of TC adsorption on PBB and M-PBB presented in Fig 3.17. From intra particle diffusion expression, values of K_i and C were calculated from the plots of q_t against $t^{1/2}$ for two materials. The intra-particle diffusion unfitted with experimental data for describing the mechanism. Because of the lower correlation coefficient on PBB and M-PBB (R^2=0.422; 0.728). When C constant from intraparticle diffusion were positive, it indicating that immediately adsorption occurred. C expresses the boundary layer thickness. M-PBB was showed the greater boundary layer effect than PBB due to larger C value. It is shown in Table 3.3. Thus, further kinetic model is used to describe the adsorption mechanism.
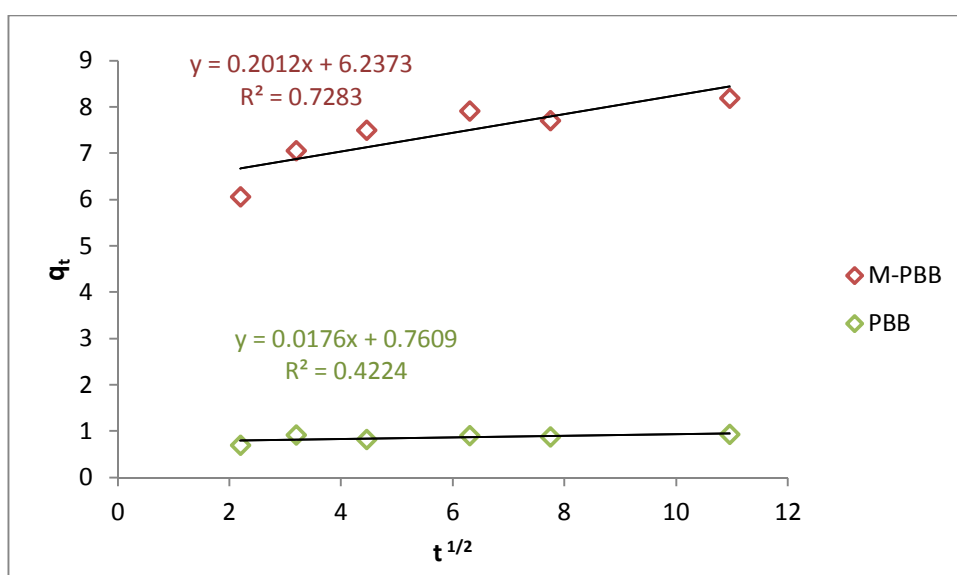
Fig 3.17 Intra-particle diffusion plots for removal of TC

d. Elovich

The Elovich model's plot of TC adsorption onto PBB and M-PBB showed in Fig 3.18. Elovich's constant values of a and b were calculated from the plots of Q_t against lnt for two materials. The correlation coefficients of PBB and M-PBB were calculated as R^2=0.515; 0.882. Elovich model was not suitable to described the adsorption mechanism of this study due to low correlation coefficients. From this model results, surface of the biochar was not energetically heterogeneous on surface.
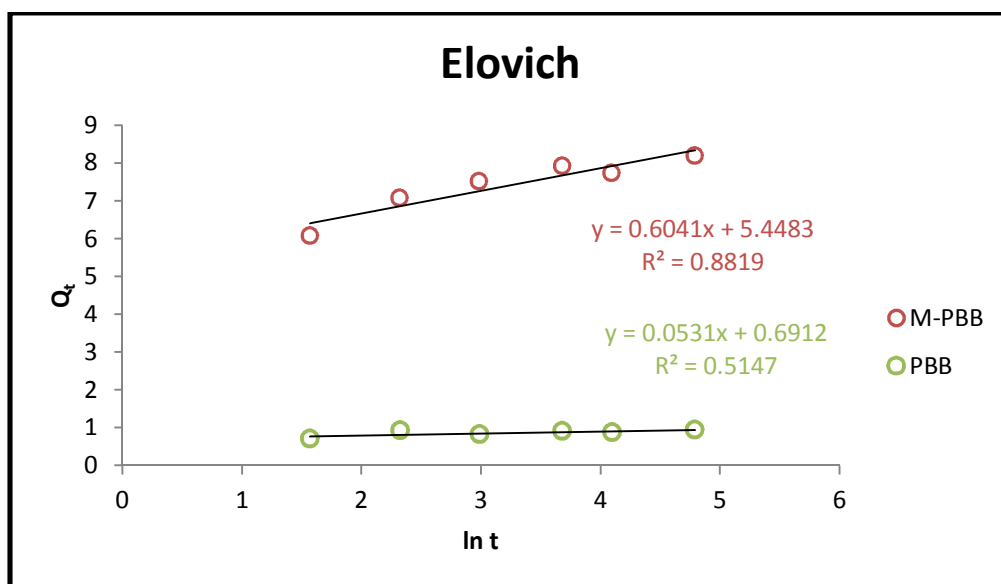
Fig 3.18 Elovich model for removal of TC onto PBB and M-PBB.

Table 3.3 Kinetic parameters for the removal of TC by PBB and M-PBB

C_0 (mg/L)	Pseudo-1st-order			Pseudo-2nd-order		
25	q_e (mg/g)	k_t (min^{-1})	R^2	q_e (mg/g)	k_2 (x 10^3 /(mg min))	R^2
PBB	1.118	-0.001	0.351	0.947	0.529	0.999
M-PBB	1.653	-0.005	0.664	8.271	0.056	0.999
	Intra-particle diffusion			Elovich		
	K_i (mg/g min$^{1/2}$)	C	R^2	a (mg/g min)	b (g/mg)	R^2
PBB	0.018	0.761	0.422	23.89×10^3	18.832	0.515
M-PBB	0.201	6.237	0.728	4.99×10^3	1.655	0.882

3.3 Adsorption thermodynamic

The thermodynamic study of TC adsorption onto M-PBB was performed to understand the energy changes at various temperatures of 20, 30, 40 and 50 ºC (293, 303, 313, 323 K). The effect of temperature on TC adsorption of batch experiment was carried out for 16 hours. It was prepared as follows: 0.04 g of M-PBB was added to each 20 mL volume of TC aqueous solution. The solution's initial concentration was 25 mg/L. The experiment's temperatures were controlled using incubator with thermostat.

K_c (Thermodynamic equilibrium constant) is calculated by q_e/C_e. According to equation (13), the ΔH^0 and ΔS^0 values can be obtained from slope and intercept of linear plots of lnK_c against $1/T$. The calculated thermodynamic values are shown in Table 3.4. ΔG^0 for the adsorption process is found as -1.639, -1.799, -2.840 and -3.645 kJ/mol at 293, 303, 313, 323 K. The values of $\Delta G°$ decreased with increasing temperature at the same TC concentration and its values were negative, indicating adsorption process is favorable and spontaneous. The enthalpy value (ΔH^0) was 19.008 kJ/mol, it indicates adsorption process is endothermic[48]. The positive value of $\Delta S°$ (69.73 J/(mol K)) indicated that the adsorption process was irreversible and favored sorption stability. This is suggesting that TC adsorption is more favorable at higher temperature.

Table 3.4 Thermodynamic parameters for the removal of TC by M-PBB

Temperature (K)	K_c	lnK_c	ΔG^0 (kJ/mol)	ΔH^0 (kJ/mol)	ΔS^0 (J/ (mol K))
293	1.959	0.673	-1.639		
303	2.042	0.714	-1.799	19.008	69.73
313	2.977	1.091	-2.840		
323	3.884	1.357	-3.645		

3.4 Comparison of adsorbents with their adsorption capacity of TC

In order to evaluate the TC adsorption capacity of M-PBB, a comparison between the maximum and equilibrium adsorption capacities obtained in this work with the reported in literature was studied. According to Table 3.5, q_e of M-PBB (15.3 mg/L) was higher than other materials such as activated carbon, bamboo charcoal, biochar R700, chitosan, rice husk ash, Fe HAP and silica oxide. Thus, M-PBB is assumed to be good adsorption material to remove the TC in water. Moreover, M-PBB can be less costly and more eco-friendly and easy to removable adsorbent for removal of TC from water.

Table 3.5 Comparison of the equilibrium and maximum adsorption capacities of TC onto various adsorbents.

Adsorbents	Adsorbate	q_e (mg/g)	q_m (mg/g) Langmuir	References
Silica oxide	TC	-	5.43	[49]
Fe HAP	TC	7.97	45.39	[11]
Activated carbon	TC	7	1.98	[30]
Rice husk ash	TC	3.41	8.37	[27]
Chitosan	TC	-	13.3	[23]
Biochar-R700	TC	10	13.85	[13]
Bamboo charcoal	TC	12	22.7	[17]
PBB	TC	2.1	-	This study
M-PBB	TC	15.3	32.2	This study
Magnetic porous carbon	TC	20.8	25.44	[50]
Ferric activated sludge	TC	40.8	87.7	[51]

CHAPTER 4

CONCLUSIONS

This study examines the possibility of TC removal using pine bark biochar (PBB) and modified pine bark biochar (M-PBB) from water. The PBB was modified with ferric and ferrous ion solution to obtain magnetic pine bark biochar. In M-PBB, the presence of iron oxide was confirmed by SEM, qualitatively determined by EDX, and quantified using DSG-TGA. The surface of PBB is revealed smooth in comparison with M-PBB. The M-PBB may become a potentially high adsorption capacity due to roughness surface with iron. Residue of PBB (9.062%) was 4 times lower than M-PBB (36.03%) due to modifying the biochar by Fe. Approximately ~27% (w/w) iron oxide was present in M-PBB.

The effect of pH, contact time, dosages and temperature on TC adsorption of PBB and M-PBB were studied. The amount of TC adsorbed (adsorption capacity) increased with increase in time and then reached equilibrium at 16 hours. The highest adsorption was observed at pH 4 to 6. Adsorption capacity was observed to decrease considerably at pH values lower than 4 and higher than pH 6. This was mainly attributed to fact that surface of adsorbent and TC molecules have similar charges at this pH range and hence electrostatic repulsion was occurring. M-PBB showed higher adsorption capacity than PBB (q_e= 2-10 mg/g). Also, the maximum adsorption capacity (q_m) of M-PBB was 15.3 mg/g on 0.5 g/L dosage at pH 6.

M-PBB was shown that adsorption is favored at higher temperature, as maximum adsorption capacity increased from 9.9 mg/g to 11.07 mg/g by increasing temperature from 293 K to 323 K. The adsorption mechanism was explained by fitting adsorption isotherms and kinetics models and determining thermodynamic parameters. A high correlation co-efficient ($R^2 \approx 0.9$) of Freundlich isotherm postulated multilayer adsorption of tetracycline on M-PBB at studied pH. The kinetic studies showed the pseudo-second-order was more suitable for indicating adsorption of TC molecules on the surface to be the rate limiting step in the process. Also, thermodynamic analysis was discovered that adsorption process is favorable, spontaneous and endothermic at studied temperature (293 – 323 K) due to the negative values of $\Delta G°$ decreased with increasing temperature. Comparison of the M-PBB and previously investigated adsorbents used for removal of TC showed that possible and good value of adsorption capacity was obtained in this study. In conclusion, M-PBB showed to have the potential for removal of TC from water as a waste, low cost and easy to removable adsorbent.

REFERENCES

1. Jarvis, W.T. Water Scarcity : Moving Beyond Indexes to Innovative Institutions. **2013**, *51*, 663–669.

2. Kivaisi, A.K. The potential for constructed wetlands for wastewater treatment and reuse in developing countries : a review. **2001**, *16*, 545–560.

3. Li, W.; Hai, X.; Han, L.; Mao, J.; Tian, M. Does urbanization intensify regional water scarcity? Evidence and implications from a megaregion of China. *J. Clean. Prod.* **2020**, *244*, 118592.

4. Maternal, W.; Infectious, H.; Migration, I.; Maternal, W.; Infectious, H.; Migration, I.; Maternal, W.; Infectious, H.; Migration, I.; Maternal, W.; et al. WHY POPULATION.

5. Mekonnen, M.M.; Hoekstra, A.Y. Four billion people facing severe water scarcity. **2016**, 1–7.

6. Pereira, L.S. by. **2002**.

7. Chen, H.; Gao, B.; Li, H.; Ma, L.Q. Effects of pH and ionic strength on sulfamethoxazole and cipro fl oxacin transport in saturated porous media. *J. Contam. Hydrol.* **2011**, *126*, 29–36.

8. Drogui, R.D.P. Tetracycline antibiotics in the environment : a review. **2013**, 209–227.

9. Jang, H.M.; Yoo, S.; Park, S.; Kan, E. Engineered biochar from pine wood : Characterization and potential application for removal of sulfamethoxazole in water. **2019**, *24*, 608–617.

10. WHO World Health Organization (WHO), Pharmaceuticals in drinking water:public health and environment water, sanitation, hygiene and health,Geneva,WHO/HSE/WSH/11.05. *Who/Hse/Wsh/11.05* **2011**.

11. Li, Y.; Wang, S.; Zhang, Y.; Han, R.; Wei, W. Enhanced tetracycline adsorption onto hydroxyapatite by Fe (III) incorporation. *J. Mol. Liq.* **2017**, *247*, 171–181.

12. Heberer, T. Occurrence , fate , and removal of pharmaceutical residues in the aquatic environment : a review of recent research data. **2002**, *131*, 5–17.

13. Wang, H.; Chu, Y.; Fang, C.; Huang, F.; Song, Y.; Xue, X. Sorption of tetracycline on biochar derived from rice straw under different temperatures. *PLoS One* **2017**, *12*, 1–14.

14. Wu, N.; Qiao, M.; Zhang, B.; Cheng, W. Da; Zhu, Y.G. Abundance and diversity of tetracycline resistance genes in soils adjacent to representative swine feedlots in China. *Environ. Sci. Technol.* **2010**, *44*, 6933–6939.

15. Wang, X.; Chen, Z.; Kang, J. Removal of tetracycline by aerobic granular sludge and its bacterial community dynamics in SBR. **2018**, 18284–18293.

16. Borghi, A.A.; Sergio, M.; Palma, A. Tetracycline : production , waste treatment and environmental impact assessment. **2014**, *50*.

17. Liao, P.; Zhan, Z.; Dai, J.; Wu, X.; Zhang, W.; Wang, K.; Yuan, S. Adsorption of tetracycline and chloramphenicol in aqueous solutions by bamboo charcoal : A batch and fixed-bed column study. *Chem. Eng. J.* **2013**, *228*, 496–505.

18. Sharma, S.; Ruparelia, J.P.; Patel, M.L. A general review on Advanced Oxidation Processes for waste water treatment. **2011**, 8–10.

19. Al-ahmad, A.; Mersch-sundermann, V. Biodegradability of some antibiotics , elimination of the genotoxicity and a ection of wastewater bacteria in a simple test. **2000**, *40*.

20. Vasconcelos, T.G.; Henriques, D.M.; König, A.; Martins, A.F.; Kümmerer, K. Chemosphere Photo-degradation of the antimicrobial ciprofloxacin at high pH : Identification and biodegradability assessment of the primary by-products. *Chemosphere* **2009**, *76*, 487–493.

21. He, L.; Dong, Y.; Zheng, Y.; Jia, Q.; Shan, S.; Zhang, Y. A novel magnetic MIL-101 (Fe)/ TiO 2 composite for photo degradation of tetracycline under solar light. *J. Hazard. Mater.* **2019**, *361*, 85–94.

22. Ahmed, M.B.; Zhou, J.L.; Ngo, H.H.; Guo, W. Science of the Total Environment Adsorptive removal of antibiotics from water and wastewater : Progress and challenges. *Sci. Total Environ.* **2015**, *532*, 112–126.

23. Chen, Y.; Shi, J.; Du, Q.; Zhang, H.; Cui, Y. Antibiotic removal by agricultural waste biochars with different forms of iron oxide. *RSC Adv.* **2019**, *9*, 14143–14153.

24. Winterbourn, C.C. Toxicology Letters Toxicity of iron and hydrogen peroxide : the Fenton reaction. **1995**, *83*, 969–974.

25. Rashed, M.N. We are IntechOpen , the world ' s leading publisher of Open Access books Built by scientists , for scientists TOP 1 %.

26. Alok Bhandari *Remediation technologies for soils and groundwater*; 2007;

27. Chen, Y.; Wang, F.; Duan, L.; Yang, H.; Gao, J. Tetracycline adsorption onto rice husk ash , an agricultural waste : Its kinetic and thermodynamic studies. *J. Mol. Liq.* **2016**, *222*, 487–494.

28. Rodríguez Correa, C.; Stollovsky, M.; Hehr, T.; Rauscher, Y.; Rolli, B.; Kruse, A. Influence of

the Carbonization Process on Activated Carbon Properties from Lignin and Lignin-Rich Biomasses. *ACS Sustain. Chem. Eng.* **2017**, *5*, 8222–8233.

29. Liu, J.; Li, E.; You, X.; Hu, C.; Huang, Q. Adsorption of methylene blue on an agro-waste oiltea shell with and without fungal treatment. *Nat. Publ. Gr.* **2016**, 1–11.

30. Liu, M.; Liu, Y.; Bao, D.; Zhu, G.; Yang, G.; Geng, J. Effective Removal of Tetracycline Antibiotics from Water using Hybrid Carbon Membranes. *Nat. Publ. Gr.* **2017**, 1–8.

31. Ji, L.; Chen, W.E.I. Mechanisms for strong adsorption of tetracycline to carbon nanotubes : A comparative study using activated carbon and graphite as adsorbents. **2009**, *43*, 2322–2327.

32. Wang, S.; Tang, Y.; Li, K.; Mo, Y.; Li, H.; Gu, Z. Bioresource Technology Combined performance of biochar sorption and magnetic separation processes for treatment of chromium-contained electroplating wastewater. *Bioresour. Technol.* **2014**, *174*, 67–73.

33. Yavuz, C.T.; Mayo, J.T.; Yu, W.W.; Prakash, A.; Falkner, J.C.; Yean, S.; Cong, L.; Shipley, H.J.; Kan, A.; Tomson, M.; et al. Low-Field Magnetic Separation of Monodisperse Fe_3O_4 Nanocrystals. *Science (80-.).* **2006**, *314*, 964 LP – 967.

34. Caminati, G.; Puggelli, M. Europium in phospholipid nanoscaffolds for the photophysical detection of antibiotic traces in solution. *Eur. Compd. Prod. Appl.* **2011**, 203–228.

35. Ghiaci, M.; Abbaspur, A.; Kia, R.; Seyedeyn-azad, F. Equilibrium isotherm studies for the sorption of benzene , toluene , and phenol onto organo-zeolites and as-synthesized MCM-41. **2004**, *40*, 217–229.

36. Foo, K.Y.; Hameed, B.H. Insights into the modeling of adsorption isotherm systems. **2010**, *156*, 2–10.

37. Kundu, S.; Gupta, A.K. Arsenic adsorption onto iron oxide-coated cement (IOCC): Regression analysis of equilibrium data with several isotherm models and their optimization. **2006**, *122*, 93–106.

38. Hu, Q.; Zhang, Z. Application of Dubinin – Radushkevich isotherm model at the solid / solution interface : A theoretical analysis. *J. Mol. Liq.* **2019**, *277*, 646–648.

39. Jang, H.M.; Kan, E. A novel hay-derived biochar for removal of tetracyclines in water. *Bioresour. Technol.* **2019**, *274*, 162–172.

40. Wu, F.; Tseng, R.; Juang, R. Characteristics of Elovich equation used for the analysis of

adsorption kinetics in dye-chitosan systems. **2009**, *150*, 366–373.

41. Kaech, A. An Introduction To Electron Microscopy Instrumentation, Imaging and Preparation. *Cent. Microsc. Image Anal.* **2002**, 1–26.

42. Ayres, P. A beginner's guide to Twitter. *ALISS Q.* **2009**, *v. 4*, no.*4*, 6–9.

43. Chiu, M.H.; Prenner, E.J. Differential scanning calorimetry: An invaluable tool for a detailed thermodynamic characterization of macromolecules and their interactions. *J. Pharm. Bioallied Sci.* **2011**, *3*, 39–59.

44. Zhou, Y.; Liu, X.; Xiang, Y.; Wang, P.; Zhang, J.; Zhang, F.; Wei, J.; Luo, L.; Lei, M.; Tang, L. Modification of biochar derived from sawdust and its application in removal of tetracycline and copper from aqueous solution: Adsorption mechanism and modelling. *Bioresour. Technol.* **2017**, *245*, 266–273.

45. Babaeivelni, K. Removal of Arsenic from Water using Manganese Oxides Adsorbents. **2014**.

46. Fierro, V.; Torné-Fernández, V.; Montané, D.; Celzard, A. Adsorption of phenol onto activated carbons having different textural and surface properties. *Microporous Mesoporous Mater.* **2008**, *111*, 276–284.

47. Peiris, C.; Gunatilake, S.R.; Mlsna, T.E.; Mohan, D. Bioresource Technology Biochar based removal of antibiotic sulfonamides and tetracyclines in aquatic environments : A critical review. *Bioresour. Technol.* **2017**, *246*, 150–159.

48. Önal, Y. Kinetics of adsorption of dyes from aqueous solution using activated carbon prepared from waste apricot. *J. Hazard. Mater.* **2006**, *137*, 1719–1728.

49. Brigante, M.; Schulz, P.C. Remotion of the antibiotic tetracycline by titania and titania-silica composed materials. *J. Hazard. Mater.* **2011**, *192*, 1597–1608.

50. Zhu, X.; Liu, Y.; Qian, F.; Zhou, C.; Zhang, S.; Chen, J. Bioresource Technology Preparation of magnetic porous carbon from waste hydrochar by simultaneous activation and magnetization for tetracycline removal. *Bioresour. Technol.* **2014**, *154*, 209–214.

51. Yang, X.; Xu, G.; Yu, H.; Zhang, Z. Bioresource Technology Preparation of ferric-activated sludge-based adsorbent from biological sludge for tetracycline removal. *Bioresour. Technol.* **2016**, *211*, 566–573.